

UNIVERSITÉ DE LIÈGE - UNIVERSITÀ DEGLI STUDI DI NAPOLI FEDERICO II



Investigation of the behavior of beam-to-column joints in seismic areas

Numerical investigation of the behavior of the panel zone

Master Thesis submitted by

JABBARI Ilyas

for the Master degree in

Ingénieur civil des constructions, à finalité approfondie

MEMBERS OF THE JURY

Pr. R. LANDOLFO
Pr. J-P JASPART
Pr. J-F DEMONCEAU
Eng. E. NUNEZ

SUPERVISORS

Pr. M. D'ANIELLO
Eng. R. TARTAGLIA
CO-SUPERVISORS
Eng. M. ZIMBRU

Academic Year 2014-2015.

Contents

| | | |
|----------|--|-----------|
| 1 | Abstract | 5 |
| 2 | Introduction | 6 |
| 3 | State of the Art | 9 |
| 3.1 | Relevant Papers | 13 |
| 4 | Literature Approach | 27 |
| 4.1 | AISC | 27 |
| 4.1.1 | Moment Resistance | 33 |
| 4.1.2 | Stiffness | 34 |
| 4.2 | Eurocode(Component Method) | 35 |
| 4.2.1 | Joint classification | 35 |
| 4.2.2 | Resistance | 38 |
| 4.2.3 | Stiffness | 48 |
| 5 | FE Validation | 55 |
| 5.1 | Model Assumption | 57 |
| 5.1.1 | Model Geometry | 57 |
| 5.1.2 | Units | 57 |
| 5.1.3 | Element type | 57 |
| 5.1.4 | Interaction | 57 |
| 5.1.5 | Material Property | 58 |
| 5.2 | Validation of the FE assumptions | 63 |
| 5.2.1 | Result Comparison | 64 |
| 6 | Parametric Study | 67 |
| 6.1 | Geometry | 67 |
| 6.2 | Web Panel Stiffeners Investigation | 69 |
| 6.2.1 | Supplementary Web Plate Influence | 74 |
| 6.2.2 | Continuity Plate Influence | 76 |
| 6.3 | Results and Comparison with the Component Method | 77 |
| 6.4 | Cost Evaluation | 82 |

| | |
|------------------------|-----------|
| 7 Conclusion | 84 |
| List of Figures | 85 |
| List of Tables | 88 |
| Bibliography | 89 |
| Nomenclature | 91 |

ACKNOWLEDGEMENT

I would like to thank everybody that contributed to the realization of this Master Thesis.

It was a wonderful experience being able to realize my Thesis abroad, in the amazing city that Naples is, to learn a new language and to be surrounded by very competent and welcoming persons.

My sincere thanks go to Pr. Raffaele LANDOLFO and Pr. Mario D'ANIELLO from the Università degli studi di Napoli Federico II, and to Pr. J-P JASPART and J-F DEMONCEAU from the Univeristé de Liege.

I thank my supervisor Roberto TARTAGLIA and my co-supervisor Mariana ZIMBRU for the time and dedication they showed me.

I would like to thank my family: my parents and my brother for their support during my Erasmus and in life in general.

Last but not least, I would like to thank my girlfriend, Annalisa EICHHOLZER, for supporting me mentally during my thesis and making my adaption in Italy easier.

STATEMENT

Steel portal frames used to be designed considering the joints either ideally pinned or fully rigid. Although this simplified the analysis and structural design process, a real and detailed understanding of the behavior of the joint was not possible. Indeed, joints in reality have all a finite stiffness and are thus semi-rigid. The joint behavior should be considered.

The codifications in Europe evolved over time and in 2005, the version published of the Eurocode 3 was exclusively dedicated to all types of joints, where the response of the joints was considered dependent of the geometrical and mechanical properties of their components by means of the component method.

However, in the Eurocode, the component method is limited to monotonic loading. Further studies in order to allow for a codified practice of beam-to-column joints submitted to seismic loading is needed.

In this paper, the results of a numerical parametric study focusing on the behavior of the column web panel zone of beam-to-column moment resisting frames in seismic area are presented. The finite element models were realized using the program Abaqus. Equal strength-double sided joints (IPE600-HEB650) are investigated under monotonic loading. The influence of the addition of continuity plates and supplementary web plates of different thicknesses is examined. Then a comparison with the results obtained from the component method is realized.

Members of the Jury:

J-F DEMONCEAU



J-P JASPART

R. LANDOLFO


E. NUNEZ

Chapter 1

Abstract

In this study, the results of a numerical parametric study on the behavior of the column web panel zone of beam-to-column moment resisting frames in seismic area are presented. Partial and Equal strength double sided joints are numerically modeled.

First, a non-exhaustive list of papers relevant to this study is presented. Then a brief review of the methods presented in the Eurocode (components method) and in the AISC (yield line theory) in order to obtain the moment-rotation curves of the joints presented here (known geometry and materials properties) is done.

Then, the description and validation of the Finite Element models used to model our joints (IPE360-HEB340, IPE450-HEB500, IPE600-HEB650) are made.

Finally, the results of the parametric study under monotonic loading of our joints are presented in order to show the influence of the different column web reinforcement methods used (continuity plates, supplementary web plate).

Dans cette étude, les résultats d'une étude numérique sur le comportement de la zone de l'âme d'une colonne dans un assemblage poutre-colonne d'un portique résistant au moment, situé dans une zone sismique, sont présentés.

Des assemblages à résistance égale et à résistance partielle sont réalisés numériquement. Tout d'abord, une liste non exhaustive des publications pertinentes à cette étude est présentée.

Ensuite, une brève révision des méthodes présentées dans l'eurocode (Méthode des composantes) et dans l'ISC (théorie de la ligne de plasticité) afin d'obtenir la courbe moment-rotation d'un assemblage est effectuée.

Puis, une description ainsi que la validation des modèles aux éléments finis utilisés pour modéliser nos assemblages (IPE360-HEB340, IPE450-HEB500, IPE600-HEB650) sont faites.

Finalement, une étude paramétrique des assemblages soumis à une charge augmentant monotoniquement est réalisée afin de montrer l'effet des différentes techniques de renforcement utilisées (Raidisseurs transversaux, doublure d'âme)

Chapter 2

Introduction

Traditionally, joints in steel portal frames were considered to be either ideally pinned (no moment is transferred) or fully rigid (moment is transferred, the relative rotation between beam and column is null). Even if it permitted a simplification in the analysis and structural design processes, a detailed understanding of the real behavior of the joint was impossible. Indeed, joints in reality do not exhibit infinite or null stiffness but all have a finite stiffness and are thus semi-rigid. It was not until the 1930's that studies on the effect of moment-rotation relationship of semi-rigid joints on steel structures began.

In the last decades, many analytical methods of semi-rigid joints were developed, from the slope-deflection equation and moment distribution methods, to matrix stiffness methods and, at present, to iterative methods coupling the global and joint structural analysis.

In 1984, the Commission of the European Community published the first version of the Eurocode 3. In this version, the joints were classified as rigid and semirigid for elastic linear analysis and with full or partial strength for elastic-plastic analysis. However, their use or the way to model them was not considered.

The Eurocode evolved and in May 2005, a new version of the Eurocode 3 was published. It was exclusively dedicated to all types of joints, where the response of the joints was considered dependent of the geometrical and mechanical properties of their components (using the component method).

All researchers agree that the joint rotational behavior should be considered. In order to do so, several models were developed to obtain the moment-rotation curve of the joint: analytical, empirical, experimental, informational, mechanical and numerical models.

According to the traditional design practices, the best way to dissipate the seismic input energy was by concentrating the dissipative zones at the beam ends and avoiding the plastic engagement of the elements constituting the connection [Mazzolani and Piluso, 1996; Bruneau et al., 1998, Faella et al., 2000].

However after the Kobe (1994) and Northridge (1995) seismic events, many concerns have raised up in the engineering community. These events revealed undesirable brittle failures in beam-to-column connections, which causes the seismic performance of such connections (welded connection) to be reconsidered.

The failure of the joint welds and premature fracture, for the Northridge case, can be attributed to the excessive distortion in the panel zone.

Brittle fractures in welded joints can generally be attributed to : Workmanship (welding defects), detailing(stress concentration at the root or toe of welds), materials (low toughness weld metal), and high seismic input (high strain rates).

In fact, the displacement/deformation are the number one cause of damage in buildings during the seismic event.

Extended bolted end-plates connections are quite popular in moment resisting joints because of their simplicity and economy in their design, fabrication and erection. Besides these advantages, bolted beam-to-column connections, in comparison to welded connections, offer an enhanced ductility (because less rigid), and a better welding quality (because performed in the shop under controlled conditions). This type of connection will be affected by many parameters such as bolt diameter, number of bolt rows and columns, bolt spacing, bolt grade, end-plate dimensions, stiffener, column and beam sizes, bolt pretension force, yield strength of steel, slip coefficient of contact surfaces, etc.

During earthquakes, a large energy dissipation of the structure is required. A structure resisting the seismic forces only in the elastic range would be very expensive. It is thus interesting to be able to use the inelastic range of a structure, provided that a correct understanding and control of the performance in the inelastic range is achieved.

There are different possibilities in order to dissipate the seismic input energy when designing a moment resisting frame in a seismic region:

- Designing the joint as full-strength joint, forcing the location of the plastic hinges at the beam ends.
- Designing the joint as partial-strength joint, forcing the dissipation of the seismic input energy in the connection.

Full strength are more expensive than partial strength. But since in partial strength connections, the joint becomes the main dissipative component, a accurate behavior assessment has to be done. It has been recognized that semi-rigid partial strength connections have dissipation and ductility capacity compatible with the seismic demand (provided a good design with an appropriate choice of the joint component where the dissipation has to occur).

It is well known that the component method (codified in Eurocode),which will

be explained in Chapter 4, allows computation of the moment-rotation response of a joint, provided that all the joint component are identified. It is very important to know that the Eurocode gives information for evaluating the monotonic behavior of beam-to-column connections, but it does not give any indication for the cyclic behavior of the joint. But the Eurocode 8 [3] opened the door to the idea of dissipating the seismic input energy in the connecting elements of beam-to-column joints.

The Eurocode 8 [3] does not allow for the yielding of the column web panel zone (the part of the column between the column flanges and the extension of the beam flanges, that transfers moment through a shear panel [5]), aiming for a 'strong panel zone-weak beam' design. However, a better understanding of the behavior of the column web panel would allow for the use the panel zone as a dissipative component (as already allowed in the American prevision)

Therefore, the use of the panel zone as a dissipative component and the ways to enhance its performance have motivated several studies on the column web panel zone, including this one.

Chapter 3

State of the Art

It is important to point out that The Eurocode 8 [3] does not allow for the yielding of the column web panel zone, aiming for a 'strong panel zone-weak beam' design. However the Eurocode achieves the total opposite by overestimating the strength of the panel zone, which as explained in [34], is due to the value considered for the shear area (too large), and to the contribution of the element surrounding the panel zone (column flanges, continuity plates if stiffened), which should not be taken into account since their contribution is fully reached only for large deformation of the panel zone, thus when it is already in the plastic range (contradictory). However allowing yielding of the column web panel zone (as in the AISC) can be beneficial, when the joint is submitted to seismic loading, in terms of energy dissipation. In this chapter, is presented an in-exhaustive list of papers published mostly about bolted end-plate steel connection, which is the type of connection investigated in this project. But also papers about other types of connections that might be relevant to the investigation of the column web panel, which is the main goal of this paper.

As explained in [18], the panel zone element is mainly a rotational spring element which transfers moment between the columns and beam framing in a joint. The moment transferred being related to the relative rotation between the columns and beams connected.

The behavior of the panel zone is extremely important under lateral loading such as seismic conditions. Indeed, in this case, the panel zone is subjected to unbalanced moment which cause shear deformation. Thus, the behavior of the panel zone has a very significant role in the overall stiffness and capacity of the frame. Indeed, depending on the type of connection, the column web panel (CWP) can supply the most important part or even the entire rotation capacity of the joint (Dubina and al, 2001)

Several previous research have showed that the panel zone has a ductile and

stable behavior, allowing concentration of inelasticity to be used in order to decrease the demand on the beams. However, large deformation of the panel zone can cause additional second-order effects and high concentration of stresses in the welds. Therefore, as mentioned in [8], the amplitude of the plastic deformation in the panel needs to be correctly evaluated and controlled.

As explained in [11] and shown by Schneider and Amidi (1998), the CWP distortions can influence by about 10% of the total lateral drift and the base shear strength by 30% in the case of regular moment resisting frame MRF. They also reported that a CWP submitted to shear develops a maximum strength significantly greater than the yielding strength (due to its strain-hardening effect), the CWP shows very good ductile behavior in the inelastic range for monotonic and cyclic loading (for the cyclic loading, the hysteretic loop is stable for large deformations), and that the maximum shear of a CWP is not easily attained due to the large interstory drift required to attain the full resistance.

As explained in [9], panel zone can be either classified in terms of strength as strong, intermediate or weak. Strong panels being able to resist the bending capacity of the adjacent beam. Weak panel zones allowing large energy dissipation within the panels. However due to the large deformations needed and the problems following from these deformations, weak panel are rarely used. On the contrary, intermediate strength panel zone allow the inelastic demands to be shared between the panel zone and the beam, which requires the panel to yield at similar load levels as those causing the flexural plastic hinges in the beams.

Several tests have been performed to investigate the load-deformation behavior of the joint panel, and the following observations were made in [18] from these tests:

- A maximum strength significantly greater than the strength at first yield is often developed in joint panel zones. This is due to strain hardening and to the contribution of the column flanges in resisting panel zone shear forces. In order to develop the maximum panel zone strength, large inelastic panel zone deformations are required.

- In both case of elastic and inelastic ranges of behavior, the panel zone deformations can have a significant contribution to the overall deformation of a SMRF (Steel moment resisting frame).

- The strength and stiffness of the panel zone can be increased by adding supplementary web plate, which effectiveness is affected by the method used to connect them to the column.

- The panel zone can have very ductile behavior in the inelastic range, for both monotonic and cyclic loading. Also, the hysteresis loops are often stable, even at

large inelastic deformations.

- Large inelastic deformations are more likely to cause brittle fracture of beam flange to column flange weld. This effect is attributed to the large localized deformations or 'kinks' in the column flanges at the boundaries of the panel zone.

As described in [13], several models can be used in order to obtain the moment-rotation curve of the joint :

Clearly, the most accurate moment-rotation curve of a joint is obtained through experimental tests. However, this technique is too expensive for everyday design practice and is usually reserved only for the field of research.

The use of a data bank is also possible, but the designer has very low chances to find the exact same joint as the one present in the data bank because of the connection typologies, geometrical properties and stiffening details of panel zone. 'SPRINT' of the European Community provides designer with tables giving the flexural strength and rotational stiffness of many different joints typologies.

Empirical models use empirical formulations obtained using regression analysis of data that can be obtained from experimental testing, parametric analysis by Finite Element (FE) models, analytical models or mechanical ones.

Analytical models are based on the basic concepts of structural analysis: equilibrium, compatibility and material constitutive relations.

Mechanical models represent a joint as a combination of rigid and flexible components (springs) with stiffness and resistance values obtained from empirical relationship. Mechanical models are very flexible and can be used for all kind of joint typologies. They take into account the non-linearity of the response by the use of inelastic constitutive laws for the spring elements

Numerical methods are commonly used for many reasons: they permit to overcome the lack of experimental results, to understand important local effects difficult to measure in reality (prying and contact forces between bolts and end-plate,...), to realize extensive parametric studies. It is possible to introduce in current Finite Element models : plasticity, large deformations, strain-hardening, instability effects, contacts between plates, and pre-stressing of bolts.

A summary of the advantages and disadvantages of each model made by Diaz et al is given in Figure 3.1 , 3.2:

| Model | Advantages | Disadvantages |
|---------------|---|--|
| Analytical | Ease of application Low computational cost | Uses simplified models Requires verification with experimental results to validate |
| Empirical | Ease of application Low computational cost | Requires calibration with other models, e.g. experimental Its applicability is limited to the connection typologies used to calibrate it Cannot be used to determine the contribution of each component of a joint to its global behaviour |
| Experimental | Best method to obtain the rotational behaviour of the joints | Very expensive to carry out |
| Informational | Can obtain information from experimental data | Large data set required to obtain good results |
| Mechanical | Applicable to any type of joint Low computational cost | The accuracy of the results depends on the number of components used and on their mechanical characteristics |
| Numerical | Can introduce local effects which are difficult to measure, (prying forces, contact, etc.) Can be used to carry out parametric studies | High computational cost |

Figure 3.1: Advantages and disadvantages of models to obtain the rotational joint behaviour.), ([13])

| Characteristics | Model | | | | | |
|---|------------|-----------|--------------|---------------|------------|-----------|
| | Analytical | Empirical | Experimental | Informational | Mechanical | Numerical |
| Advanced analysis available (contact, pretension, etc.) | Low | Low | Medium | Low | Medium | High |
| Level of complexity | Low | Low | Medium | Medium | Medium | High |
| Database requirements | High | High | Low | High | Low | Medium |
| Cost | Low | Low | High | Medium | Low | Medium |
| Reusable for other connection typologies | No | No | No | No | Yes | Yes |
| Parameterization | Low | Low | Low | High | Medium | High |
| Solution time | Low | Low | High | Low | Low | Medium |
| User skills | Low | Low | Medium | Medium | Medium | High |
| Usability for design optimization | Low | Low | N/A | High | High | High |
| Match real behaviour | Low | Low | High | Medium | Medium | Medium |
| Provides extra information | No | No | Yes | No | Yes | Yes |

N/A not applicable.

Figure 3.2: Principal characteristics of current models to obtain the rotational behaviour of a joint.), ([13])

3.1 Relevant Papers

Many papers relevant to this study have been published before (Numerical, analytical and experimental studies):

- In [7], Bursi and Jaspart presented part of a study devoted to the analysis of bolted steel connections by means of finite elements and concluded that the comparison between computed and measured values in each phase of their work highlighted the effectiveness and degree of accuracy of the proposed FE models.
- As concluded in [8], Castro and Al. presented a new approach for representing the panel zone component in steel and composite moment resisting frames. The contribution of the column flanges to the extra resistance of the panel zone is accounted for. The procedure considers both shear and bending deformations, and addresses the elastic and inelastic stages. The comparison with available experimental results coupled with detailed numerical simulations showed good accuracy and reliability of the method. As explained in [8]. Usually, The panel is typically assumed to have rigid boundaries and to behave under pure shear stress state. This simplification allows the conversion of the bending moment into horizontal forces, which leads to a set of simple analytical expressions for the idealized springs. It is also considered that beyond yielding of the panel, the shear stiffness provided by the column web effectively drops to that corresponding to strain-hardening of the material. Additional study to account for the contribution of the Continuity plates to the extra resistance of the panel zone would also be of good concern.
- In [9], Castro et al reviewed the various approaches for panel zone design available in Europe and in the U.S.. They did a numerical study in order to investigate the influence of a number of parameters on the inelastic response of the structure. The limitations of the Eurocode concerning the web panel zone were pointed out. Indeed, an overestimation of the panel zone capacity in Eurocode 3 leads to quite weak panel zones (Despite the stated objective of achieving relatively strong panel zone). Castro et al showed that the Eurocode overestimates the contribution of the column flanges to the shear capacity by not taking into account the initial stress state in the column flanges before these components are mobilized in the response, and considering the full plastic capacity of the column flanges. A comparison with the AISC showed that the contribution of the column flanges according to Eurocode 3 is twice that of the U.S. provisions. However, also the US codes, weak panel zone is achieved through design. They highlighted the benefits of adopting a balanced design for panel zones

(for relatively low gravity loads).

Nevertheless, further numerical studies (supported by experimental tests) in order to have a more reliable codified design approach in terms of earthquakes are encouraged.

Also as pointed out in [9], they did not consider the uncertainty in terms of material strength, which thus needs further investigation.

- In [10], it was stated that the use of partial-strength joints in MRF structures located in seismic regions is allowed by Eurocode 8 under specific circumstances: If the connection is the main dissipative component of the frame, they have to be checked by advanced calculations, not present in the codes, and demonstrated by experimental tests. As pointed out by Castro et al, these kinds of joint require more research to find alternative solutions to implement in future codes of practice. In [10], the study of cyclic and dynamic behavior of the partial-strength beam-to-column connections using numerical simulations based on the FE program ABAQUS was realized. The geometry of the connections tested are shown here after as well as the failures modes of the different configurations:

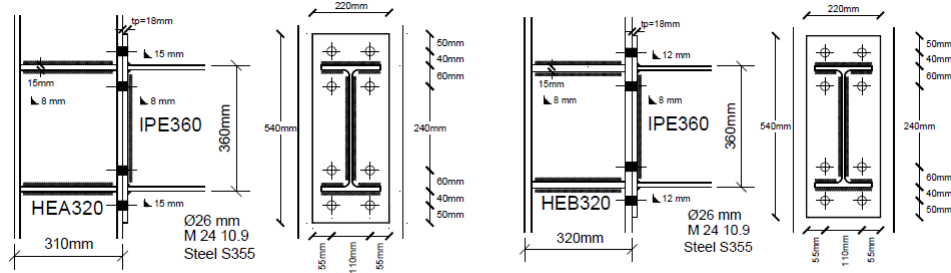


Figure 3.3: Geometries of J1 and J3 series), ([10])

| Con. | % of $M_{b,Rd}$ [10] | Description |
|------|----------------------|---|
| C1 | 92% | J3.2 [6] |
| C2 | 121% | C1 modified, strengthening the web and the end-plate (EC3) |
| C3 | 76% | Based on C2, reduction of the column strength (HEA320), failure mode column web panel in shear |
| C4 | 76% | Based on C2, reduction of the end-plate, failure mode 1 (EC3) |
| C5 | 76% | Based on C2, reduction of the end-plate, failure mode 2 (EC3) |

Figure 3.4: Connections chosen for the EVD determination), ([10])

A Direct Displacement-Based Design is presented in this paper for the desing is seismic regions. However, in our case, an investigation on the extension

of the component method for seismic design would be more appropriate.

- In [11], the influence of the different column web stiffening solutions on the performance of the joints of MRF was experimentally investigated. A quasilinear relationship between the moment capacity and the total shear area of the web panel resulted from these tests (Ignoring the limitations specified in the Eurocode 3 allowing only one SWP to be taken into account). On the other hand, the initial rigidity has increased non-proportionally with the shear area. For specimens with web reinforcement, fragile failure modes have been achieved. It was shown that the hardening stiffness of cyclic tests increases with the shear area. They tested 5 different specimens. The description of the CWP tests and the cyclic behavior and failures modes are shown in Figures 3.5 , 3.6, 3.7

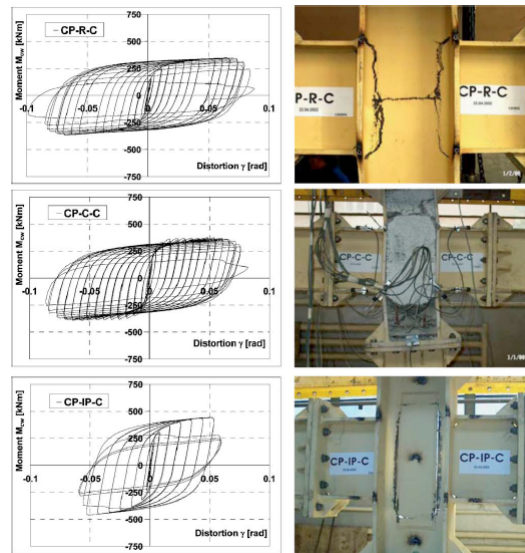


Figure 3.5: Cyclic behavior and failure mode of cyclic specimens, 1), ([11])

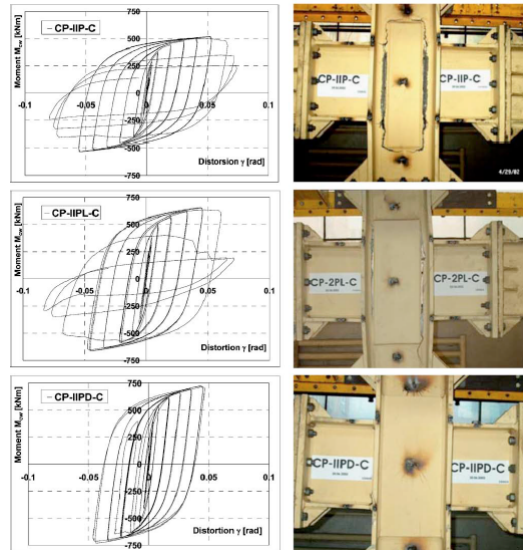


Figure 3.6: Cyclic behavior and failure mode of cyclic specimens, 2), ([11])

| Test reference | Reinforcing type | Sketch | Width of the doubler plates | Loading type |
|----------------|------------------|--------|-----------------------------|---------------|
| CP-R-M | None | | --- | Monotonic |
| CP-R-C | | | | Cyclic - ECCS |
| CP-C-M | Concrete | | --- | Monotonic |
| CP-C-C | | | | Cyclic - ECCS |
| CP-IP-M | Doubler plates | | 150 mm | Monotonic |
| CP-IP-C | | | | Cyclic - ECCS |
| CP-IIP-M | Doubler plates | | 150 mm | Monotonic |
| CP-IIP-C | | | | Cyclic - ECCS |
| CP-IIPL-M | Doubler plates | | 220 mm | Monotonic |
| CP-IIPL-C | | | | Cyclic - ECCS |
| CP-IIPD-M | Doubler plates | | 260 mm | Monotonic |
| CP-IIPD-C | | | | Cyclic - ECCS |

Figure 3.7: Description of the CWP Tests), ([11])

They showed that for the cyclic tests, specimens showed very stable behavior for all the cases, having their resistance increasing proportionally to the shear area. They also showed good ductility and strain-hardening ratios. They also pointed out that failure was brittle in the case of stiffened specimens, however this occurred at relatively high values of plastic distortion. Further confirmation of the observations made on these tests would be adequate by means of numerical studies calibrated on these experimental results. These additional numerical studies would also permit numerous other strengthening configuration of the web panel to be analyzed. Finally, welded connection were tested in this paper, an additional study for bolted connection would be quite relevant to our study.

- In [12], full three dimension FE models of steel beam to column bolted extended end-plate joints are presented in order to obtain their behavior (Including contact and sliding between elements, bolt pre-tensioning, geometric and material non-linearity). It was presented that the rotational deformation of the joint Φ_j is the sum of the shear deformation of the column web panel zone γ and of the connection rotational deformation θ_c . As concluded in [12], the validation process revealed that the FE model was able to accurately predict the failure mode of the joint, while underestimating the initial rotational stiffness and both overestimating and underestimating the design moment resistance. These differences being attributed to :
 - The residual stresses in the welds (not considered in the FE model)
 - The tolerances in the dimensions of the sections and the geometrical imperfections in the experimental results used to validate and calibrate the FE model.
 - The approximation used in incorporating the material stress-strain relationship into the FE model
 - Errors in determining the experimental initial rotational stiffness.

The study also showed that material work hardening and contact parameters (normal penalty stiffness factor and elastic slip factor) are the parameters that have the biggest effect on the behaviour of the joint.

Further studies considering different types of strengthening of the connection (Continuity plates, supplementary web plate, ribs,...) would be interesting to investigate, as well as the FE validation of the cyclic behavior of the connections tested. Finally, double sided connections submitted to anti-symmetric loading would also be relevant to our study.

- In [13], the several models that can be used to obtain the moment-rotation curve of a joint are very well presented: analytical, empirical, experimental, informational, mechanical and numerical. Special attention is given to the

component method (valid only for joints subjected to pure bending, the method fails if an axial load is also present).

The different moment-rotation curves (linear, bi-linear, multi-linear and non-linear) that can be used depending on the type of global structural analysis required are presented. As mentioned in [13], the most accurate being the nonlinear one, although the multi-linear representation is commonly used for mechanical models.

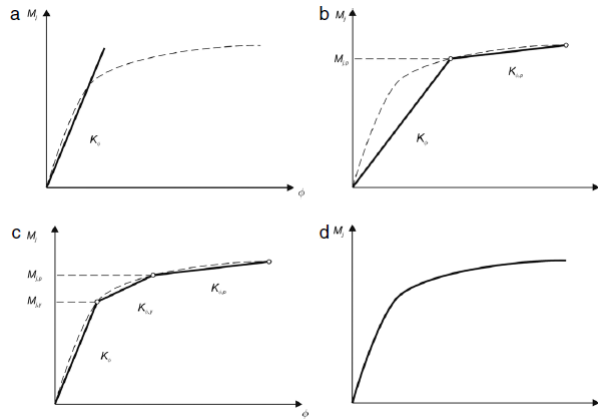


Figure 3.8: Different mathematical representations of the $(M_j - \Theta)$ curve: (a) linear; (b) bi-linear; (c) multi-linear (tri-linear); (d) nonlinear.), ([13])

Although the mechanical method (component method) presented here has been proven to be applicable for every kind of joints submitted to monotonic loading. Research is still going on in order to extend the use of the method for cyclic solicitations.

- In [14], two series of six double-sided joints with three different beam-to-column connection typologies (extended end-plate, welded, with cover plates) have been experimentally tested under symmetrical and antisymmetrical cyclic loading. Dubina et al showed that the antisymmetrical loading (as in earthquakes) triggers the participation of the panel zone to plastic mechanism, which causes increase of ductility, decrease of moment capacity and initial stiffness and more stable energy dissipation through hysteretic loop, compared to the symmetric loading. Dubina et al made precise descriptions of the failures occurring at the different cycles of the tests for the different configurations. When comparing to Eurocode 3, they remarked that the antisymmetrical loading has led to a 50% drop of the theoretical joint plastic moment with respect to the plastic moment of the connecting beam, due to the web panel in shear.

Figure 3.9 shows the moment-rotation envelopes of the different joint tested

and Figure 3.10 shows a comparison between experimental and computed curve.

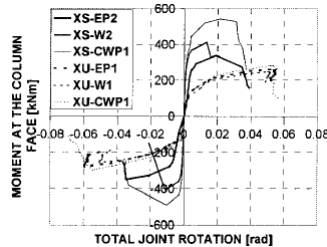


Figure 3.9: Moment-Rotation Envelopes, ([14])

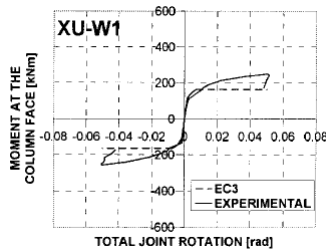


Figure 3.10: Comparison between Experimental and Computed Curves, ([14])

They also concluded that it is necessary to use an appropriate model for double-sided beam-to-column joints capable of reflecting the different behavior of these joints under gravitational and earthquake loading. Indeed, a joint classified as rigid and full strength under symmetrical loading may become partially resistant and semi-rigid under anti-symmetrical loading. Dubina et al demand for a more realistic modeling of the joint behavior to be supported by detail design provisions of Eurocode 3. The only one supported (although 2 models are mentioned) in the Eurocode 3 being the simplified modeling representing each joint as a separate rotational spring to take into account the behavior of the web panel. This causing 2 sets of moment-rotation characteristics for 2 types of loading for the same joint configuration, creating difficulties when implementing into structural analysis programs because it will not reflect the real joint behavior under different loading type. The actual behavior of the joint as shown in Figure 3.11 (a) should be used instead.

Dubina et al concluded that bolted end-plate connections showed good rotation capacity and more ductile behavior compared to welded connections,

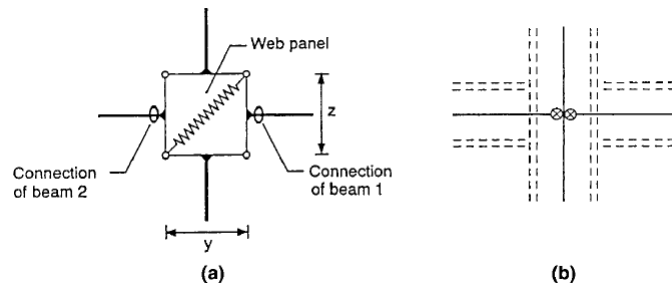


Figure 3.11: Joint Modeling Reflecting (a) Actual Behavior and (b) Simplified Modeling, ([14])

although they have a smaller initial stiffness. They should be designed as to prevent brittle failure by bolt rupture (which can be prevented by a bolt overstrength design). Loosening of bolts during cycle reversals caused stiffness degradation.

Another experimental study of connection with strengthening of the web panel zone with supplementary web plate would be interesting. This in order to see if SWP could change the weakest component of the connection when submitted to antisymmetric loading. It would also be important to realize cyclic tests of these connections.

- In [15], it has been shown that the parameters describing the rotational behavior of extended end-plate connection (strength and stiffness) are related to each other, and they can be calculated on the basis of important geometrical parameters such as m/d ratio, end-plate thickness and column flange thickness. Finally it has been concluded that allowing a semi-rigid solution (in comparison with a pinned solution), the increase in cost due to detailing of beam-to-column joints is about 5% while the economy in terms of overall cost of the structure can reach 10% and more.
A study in terms of economical benefits considering stiffened joints would also be significant.
- In [18], analytical models are presented to predict the elastic and inelastic response of the panel zone of the column. The models used are based on the concepts of representing the panel zone as a nonlinear rotational spring. The model for monotonic loading is based on quadri-linear panel zone moment-deformation relations (both bending and shear deformation modes are considered). While the model for cyclic loading is based on Dafalias' bounding surface theory combined with Cofie's rules for movement of the bound line. Some issues in the models used appeared: The effect of very thick column flanges on panel zone strength needs further experimental data to be bet-

ter accounted for; The effectiveness of supplementary web plate also needs additional studies in order to better quantify the contribution of the SWP to the panel zone strength and stiffness for different attachment details (one side, both sides, welding details, etc). Finally, the models presented in [18], though they account for material yielding and strain hardening, need further studies in order to be able to predict strength degradation due to instability (shear buckling) or fracture of the column or beam flanges at the corner of the panel zone.

- A very important work was presented in [19], indeed, an experimental research focusing on the possibility of using the component method in the prediction of the cyclic rotational response of beam-to-column joints, knowing their geometrical and mechanical properties, was carried out. In order to do so, they focused on the experimental evaluation of the force vs. displacement cyclic response of all the joint components. Iannone et al classified the different components in terms of dissipation capacity (all components subjected to compression that could be non dissipative because of instability (buckling) or brittle failures such as bolt or weld failure have to be avoided).

| Component | Dissipative | Non dissipative |
|----------------------------|-------------|-----------------|
| Web panel in shear | x | |
| Column web in compression | | |
| <i>Crushing resistance</i> | x | |
| <i>Buckling resistance</i> | | x |
| Column web in tension | x | |
| Column flange in bending | | |
| <i>Welded joints</i> | | x |
| <i>Bolted joints</i> | x | |
| Endplate in bending | x | |
| Beam web in tension | x | |
| Plate in tension | x | |
| Plate in compression | | |
| <i>Crushing resistance</i> | x | |
| <i>Buckling resistance</i> | | x |
| Bolts in tension | | x |
| Bolts in shear | | x |

Figure 3.12: Identification of dissipative components, ([19])

They tested 4 specimens, that have been designed to have the same flexural strength but different weakest joint component, leading to different values of rotational stiffness and plastic rotational supply [19]:

- EEP-CYC 01 is a partial strength extended end-plate joint having the panel zone as weakest joint component.
- EEP-CYC 02 is a partial strength extended end-plate joint having the end-plate in bending as weakest joint component.
- EEP-DB-CYC 03 is a full strength extended end-plate joint designed forcing the development of plastic hinge in the beam by cutting the beam flanges following the design criteria for the reduced beam section (RBS) strategy.
- TS-CYC 04 is a partial strength joint with a couple of T-stubs bolted to the beam flanges and to the column flanges and designed to be the main source of plastic deformation capacity.

Iannone et al concluded from their experimental results that the overall energy dissipation capacity of joints can be obtained as the sum of the energy dissipated by the single components (See Figure 3.13 and 3.14 as example of sample EEP-CYC 01). Which assures the extension of the component method to the cyclic response of beam-to-column joints, as long as the joint components are correctly identified and their cyclic force vs displacement behavior correctly modeled.

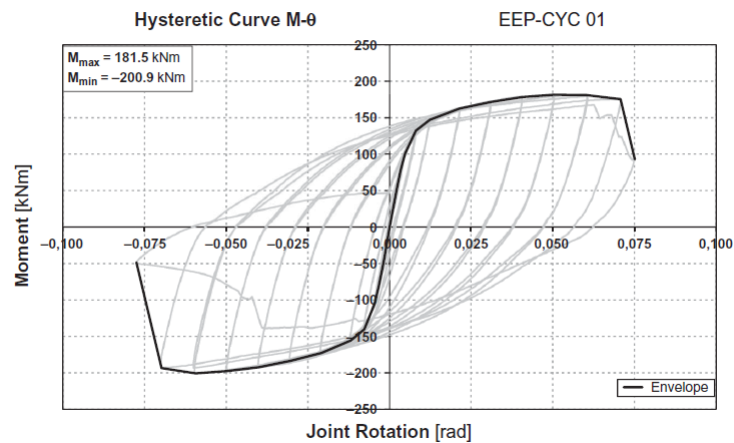


Figure 3.13: EEP-CYC 01 Moment-Rotation curve, ([19])

Further validation of this study on several joint configurations, and additional and experimental tests in order to implement the use of the method in the Eurocode are required.

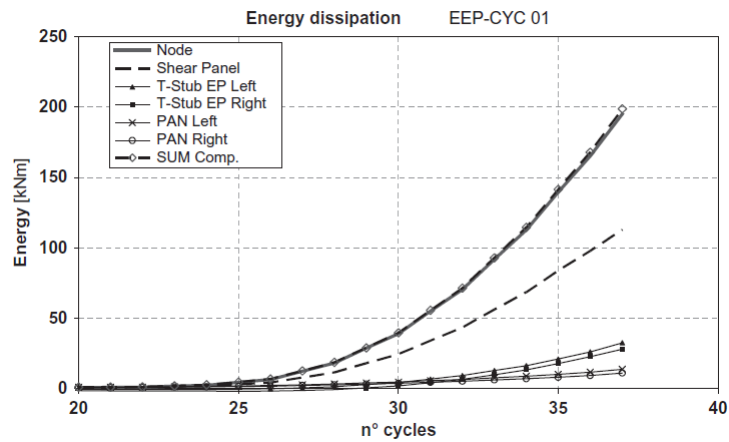


Figure 3.14: Energy dissipation of specimen EEP-CYC 01, ([19])

- In [20], Latour et al developed a mechanical model for predicting the cyclic response of bolted joints starting from models available in the literature. The model relies on the component method just as in the companion article [19]. They obtained very encouraging results in order to predict accurately the cyclic response of bolted connection using the component method, as shown in Figure 3.15. However, as concluded in [20], the accuracy of the developed mechanical model can be improved by additional test results on the cyclic response of isolated joint components which allow better modeling of the cyclic force vs displacement behavior of the joint components. For example, a T-stub calibrated on the cyclic response of welded T-stubs gives better results in the modeling of the end-plate in bending while a T-stub calibrated on the cyclic response of rolled T-stubs gives better results in the modeling of the column flange in bending. Finally, tests with other loading history than a symmetrical one would allow the cyclic model relying on empirical parameters to be better calibrated for any loading history.

| Joint | Typology | $E_{diss,mod}$ [kNm] | $E_{diss,exp}$ [kNm] | $E_{diss,mod}/$ $E_{diss,exp}$ [kNm] |
|--|-------------------|-------------------------|-------------------------|---|
| EEP-CYC 01 (Iannone <i>et al.</i> , 2010) | Extended endplate | 210 | 197 | 1.07 |
| J-1.3 (Kim and Yang, 2006) | Extended endplate | 299 | 292 | 1.02 |
| FW (Nogueiro <i>et al.</i> , 2006) | Fully welded | 60 | 64 | 0.94 |
| EEP-CYC 02 (Iannone <i>et al.</i> , 2010) | Extended endplate | 67 | 58 | 1.15 |
| TS-CYC 04 (Iannone <i>et al.</i> , 2010) | Extended endplate | 154 | 139 | 1.10 |
| FPC/B (Bernuzzi <i>et al.</i> , 1996) | Flush endplate | 43 | 42 | 1.04 |

Figure 3.15: Comparison between model and experimental dissipated energy, ([20])

- In [21], an analytical procedure for the estimation of the behavior of unstiffened extended end-plate connections has been presented. This method (similar to the one in AISC) which is based on the theory of yield line mechanism allows the determination of the yielding and ultimate moment stiffness of the connection, knowing the geometrical and material properties. However, the yield line theory has the problem of not being adaptable for the design of any joint geometry.
- In [23], Shi et al tested 8 full-scale structural beam-to-column end-plate moment connection under earthquake loading. As done in [23], the following conclusions could be made:
 - The extension of the end-plate on both side can provide the strength, rotational stiffness, ductility and energy dissipation needed in seismic moment frames, compared to the flush end-plate connection whose hysteretic loop pinches significantly and its stiffness degrades, indicating a non-adequate energy dissipation capacity.
 - For end-plate connections, the $M - \Phi$, $M - \Phi_s$, $M - \Phi_{ep}$ curves under monotonic loading can be considered as the envelope line of the corresponding hysteretic curves under cyclic loading. (The total deformation of the connection Φ can be considered as the sum of the deformation due to shear Φ_s and the deformation of the End-Plate Φ_{ep} , see Figure 3.17)
 - Details of end-plate connection have been given for seismic frames in [23]
 - 3 failure modes (Failure of end-plate and column flange; yielding of panel zone prior to the end-plate and the bolts; failure of the end-plate prior to the bolts) requirements and corresponding calculation method have been

proposed.

- The hysteric moment-rotation model for the end-plate connection extended on both sides has been recommended (see Figure 3.16).

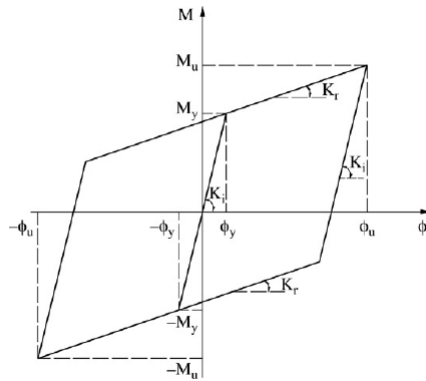


Figure 3.16: Hysteretic moment-rotation ($M - \Phi$) model of the extended end-plate connection, ([23])

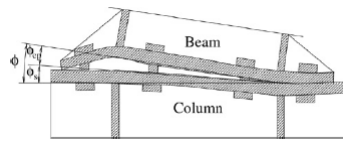


Figure 3.17: Joint rotation definition , ([23])

- Shi et al tested in [25] 5 full-scale joint (stiffened and extended beam-to-column end-plate connection) in order to investigate the influence of bolt size and end-plate thickness on the joint behavior. The complete loading process of each component (panel zone, bolt, end-plate, column flange) was analyzed. Shi et al developed an analytical method to evaluate the moment-rotation ($M - \Phi$) relationship of these connections. This method is also able to provide the moment-shear rotation ($M - \Phi_s$) and moment-gap rotation ($M - \Phi_{ep}$). This analytical method compared to the tests made gave accurate results.

Further studies on cyclic tests would be very interesting.

Chapter 4

Literature Approach

4.1 AISC

In the AISC [4], a complete design procedure for the four bolt unstiffened, four bolt stiffened and eight bolt stiffened end-plate moment connections is explained. In this paper, we will focus only on the design procedure given in the AISC for the four bolt stiffened endplate moment joint for an unstiffened and a stiffened column. However, since we know already the connection geometry and material properties of our joints, we will present the verification that has to be made in order to verify that our connection design respects the rules of the AISC and in fine obtain the moment-rotation curve. The connection geometry is shown in Figure 4.1:

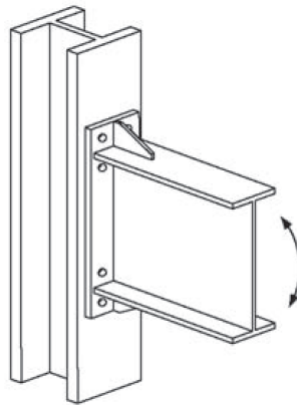


Figure 4.1: Four-bolt stiffened configuration, (*Chapter 6, [4]*)

The design procedure for extended end-plate moment connections subject to cyclic loading is based on 4 points:

- The required connection design moment
- Connection bolt strength
- End plate strength
- Column flange bending strength

The procedure uses the yield-line theory for the determination of the end plate strength and the column flange flexural strength, and a simplified method to determine the bolt forces. The following procedure is recommended for bolted end-plate moment connection subject to cyclic/seismic forces.

AISC Procedure

Figure 4.2 shows the geometry of the connection:

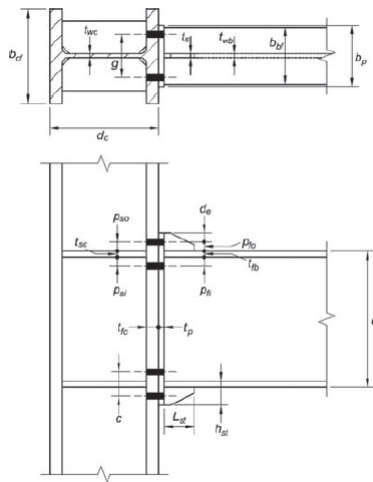


Figure 4.2: Four-bolt stiffened geometry, (*Chapter 6, [4]*)

Bolts and end-plate

- The no prying bolt strength moment of the bolts is obtained from equation (4.1) :

$$\Phi M_{np} = 2 * \Phi * P_t * (h_0 + h_1) \quad (4.1)$$

Where

$$P_t = F_t * A_b$$

$$A_b = \frac{\pi * d_b^2}{4}$$

$$\Phi = 0.75$$

-We can compute the end plate flexural strength from equation (4.2):

$$\Phi M_{pl} = \Phi_b * F_{yp} * t_p^2 * Y_p \quad (4.2)$$

Where

$$\Phi = 0.75$$

$$\Phi_b = 0.9$$

| End-Plate Geometry and Yield Line Pattern | | Bolt Force Model |
|--|---|------------------|
| Case 1 ($d_e \leq s$) | Case 2 ($d_e > s$) | |
| | | |
| Case 1 ($d_e \leq s$) | $Y_p = \frac{b_p}{2} \left[h_1 \left(\frac{1}{\rho_n} + \frac{1}{s} \right) + h_0 \left(\frac{1}{\rho_n} + \frac{1}{2s} \right) \right] + \frac{2}{g} [h_1(\rho_n + s) + h_0(d_e + \rho_n)]$ | |
| Case 2 ($d_e > s$) | $Y_p = \frac{b_p}{2} \left[h_1 \left(\frac{1}{\rho_n} + \frac{1}{s} \right) + h_0 \left(\frac{1}{s} + \frac{1}{\rho_n} \right) \right] + \frac{2}{g} [h_1(\rho_n + s) + h_0(s + \rho_n)]$ | |
| $s = \frac{1}{2} \sqrt{b_p g} \quad \text{Note: If } \rho_n > s, \text{ use } \rho_n = s.$ | | |

Figure 4.3: Summary of Four-Bolt Extended Stiffened End-Plate Yield Line Mechanism Parameter, (*Chapter 6, [4]*)

- We need to calculate the factored beam flange force that will be transmitted from the beam to the connection. If we consider no normal forces acting on the beam, we have:

$$F_{fu} = \frac{M_{uc}}{d_b - f_{fb}} \quad (4.3)$$

- Using a stiffened end-plate, the yielding and rupture resistance of the extended portion of the end-plate do not have to be verified. However, we have to verify that the stiffener has the minimum thickness required:

$$t_{s,req} = t_{wb} * \frac{F_{yb}}{F_{ys}} \quad (4.4)$$

Also, in order to verify that no local buckling of the stiffener plate occurs, the following criterion must be satisfied:

$$t_s \geq 1.79 * h_{st} * \sqrt{\frac{F_{ys}}{E}} \quad (4.5)$$

The stiffener-to-beam flange and stiffener-to-end plate welds must also be verified. Indeed they have to be able to develop the stiffener plate in shear at the beam flange and in tension at the end plate. For this purpose, either fillet or complete joint penetration (CPJ) welds are needed for the beam flange welds. For the stiffener-to-end plate weld, CPJ should be used for stiffener thickness greater than 3/8 in (9.525 mm) and fillet welds for thickness less or equal to 3/8 in (9.525 Mm).

- The bolts have to be verified in both shear rupture and bolt bearing/tear out failure of the end-plate and column flange. The bolt shear rupture strength of the joint is conservatively considered to be provided by the bolts at the compression flange:

$$R_n = \Phi * n_b * F_v * A_b > V_u \quad (4.6)$$

Where

$$\Phi = 0.75$$

- Bolt bearing and tear out failure of the end plate and column flange is verified by:

$$R_n = \Phi * n_i * R_{n(\text{InnerBolts})} * \phi * n_o(\text{Outerbolts}) > V_u \quad (4.7)$$

Where

$$\Phi = 0.75$$

$$R_n = 1.2 * L_c * t * F_u < 2.4 * d_B * t * F_u, \text{ for each bolt}$$

$$t = t_c \text{ or } t_{ep}$$

For our joint configurations, welds are considered to be full penetration.

Column side

- The column flange flexural strength is given by equation (4.8):

$$\Phi M_{cf} = \Phi_b * F_c * t_c f^2 * Y'_p \quad (4.8)$$

Where

$$\Phi = 0.75$$

$$\Phi_b = 0.9$$

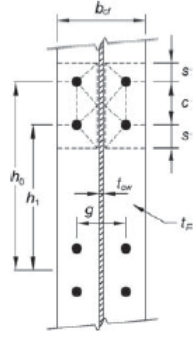
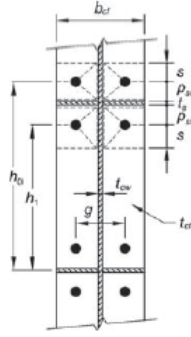
| Unstiffened Column Flange Geometry and Yield Line Pattern | Stiffened Column Flange Geometry and Yield Line Pattern |
|---|--|
|  |  |
| <p>Unstiffened Column Flange</p> $Y_c = \frac{b_{cf}}{2} \left[h_1 \left(\frac{1}{s} \right) + h_0 \left(\frac{1}{s} \right) \right] + \frac{2}{g} \left[h_1 \left(s + \frac{3c}{4} \right) + h_0 \left(s + \frac{c}{4} \right) + \frac{c^2}{2} \right] + \frac{g}{2}$ $s = \frac{1}{2} \sqrt{b_{cf} g}$ | <p>Stiffened Column Flange</p> $Y_c = \frac{b_{cf}}{2} \left[h_1 \left(\frac{1}{s} + \frac{1}{\rho_{sl}} \right) + h_0 \left(\frac{1}{s} + \frac{1}{\rho_{so}} \right) \right] + \frac{2}{g} \left[h_1 (s + \rho_{sl}) + h_0 (s + \rho_{so}) \right]$ $s = \frac{1}{2} \sqrt{b_{cf} g} \quad \text{Note: If } \rho_{sl} > s, \text{ use } \rho_{sl} = s.$ |

Figure 4.4: Summary of Four-Bolt Extended Column Flange Yield Line Mechanism Parameter, (*Chapter 6, [4]*)

- We have to verify both unstiffened and stiffened column. Therefore, in case of stiffeners, we need to calculate the required stiffener force.

The equivalent column design force is given by :

$$\phi * R_n = \frac{\phi * M_{cf}}{(d_b - t_{fb})} \quad (4.9)$$

- The unstiffened local column web yielding strength at the beam flange is given by equation (4.10):

$$\phi * \mathbf{R}_n = \phi * C_t * (6k_c + N + 2t_p) * F_{yc} * t_{wc} > \mathbf{F}_{fu} \quad (4.10)$$

Where

$$\phi = 1.0$$

$C_t = 1$ because the distance from the column top to the top face of the beam flange is more than the depth of the column

- The column web buckling strength of the unstiffened column web at the beam compression flange is given from equation (4.11):

$$\phi * \mathbf{R}_n = \frac{\phi * 24 * t_{wc}^3 * \sqrt{E * F_{yc}}}{h} > \mathbf{F}_{fu} \quad (4.11)$$

Where

$$\Phi = 0.9$$

- The unstiffened column web crippling strength at the beam compression flange is given by equation (4.12):

$$\phi * \mathbf{R}_n = \Phi 0.80 t_{wc}^2 [1 + 3 \left(\frac{N}{d_c} \right) \left(\frac{t_{wc}}{t_{fc}} \right)^{1.5}] \sqrt{\frac{E F_{yc} t_{fc}}{t_{wc}}} \quad (4.12)$$

Where

$$\Phi = 0.75$$

- If the column is stiffened with continuity plates, the required strength for them is given by :

$$\mathbf{F}_{su} = \mathbf{F}_{fu} - \min(\Phi \mathbf{R}_n) \quad (4.13)$$

Where $\min \Phi R_n$ is the minimum design strength value from the column flange bending, column web yielding, column web buckling and column web crippling strengths.

- Finally shear yielding and plate buckling strength of the column web panel zone must be checked according specification in [Seismic Provisions for Structural Steel Buildings (AISC, 2002)]. The use of equation 4.14 and 4.15 applied when frame stability, including plastic panel-zone deformation, is considered in

the analysis. These equations take into account the additional inelastic shear strength available in a connection with adequate ductility. This inelastic shear strength is often used for the design of frames in high seismic zones:

For $P_r \leq 0.75P_c$

$$\mathbf{R}_n = 0.60F_y d_c t_w \left(1 + \frac{3b_{cf} t_{cf}^2}{d_b d_c t_w}\right) \quad (4.14)$$

For $P_r > 0.75P_c$

$$\mathbf{R}_n = 0.60F_y d_c t_w \left(1 + \frac{3b_{cf} t_{cf}^2}{d_b d_c t_w}\right) \left(1.9 - \frac{1.2P_r}{P_c}\right) \quad (4.15)$$

Where

$$P_c = P_y \text{ [N] (LFRD)}$$

$$P_y = F_y A_c$$

4.1.1 Moment Resistance

As mentioned earlier, as we already know the end-plate geometry, bolt diameter, beam and column geometry, and material properties, we can obtain the moment strength (if the procedure criteria are respected) , ΦM_n , according to the AISC, by :

- Calculating the end-plate bending strength, the column flange bending strength, and the no-prying bolt tension rupture strength, as explained before.
- Determining the behavior of the end-plate and column flange, being 'thick' or 'thin', using the following equations:

For the end-plate

$$\text{If } M_{pl} > 1.1M_{np} \rightarrow \textit{Thickplate}$$

$$\text{If } M_{pl} < 1.1M_{np} \rightarrow \textit{Thinplate}$$

For the end-plate

$$\text{If } M_{cf} > 1.1M_{np} \rightarrow \textit{Thickflange}$$

$$\text{If } M_{cf} < 1.1M_{np} \rightarrow \textit{Thinflange}$$

Thus, if both the end-plate and the column flange have thick plate behavior, then the connection design strength, is equal to the no prying bolt strength, ΦM_{np} . Otherwise, in case of thin plate behavior, the connection does not meet the requirements of the procedure presented. An additional limit state, bolt rupture

with prying, is induced by the thin plate behavior, whose computation is available in [AISC/MBMA Design Guide 16 Flush and Extended Multiple-Row Moment End-Plate Connections (Murray and Shoemaker, 2002)].

4.1.2 Stiffness

In the AISC specifications, no procedure is described in order to calculate the stiffness of the joint. The connections are assumed either fully rigid or pinned.

4.2 Eurocode(Component Method)

In the past, when designing steel portal frames, it was assumed that their beam-to-column joints were ideally pinned or fully rigid. With pinned joints, no moment is transmitted between the beam and the column, only axial and shear forces can be transferred. This means that they have no rotational stiffness. On the contrary, fully rigid joints have a rotational compatibility, which means that the relative angle deformation between the beam and the column is null. They are able to transmit axial, shear and moment. Considering the connections pinned or fully rigid decoupled the analysis of the joints from the analysis of the structure. It had the effect of simplifying the analysis and structural design process but prevented a detailed understanding of the behavior of the joints. Indeed, joints being in reality semi-rigid and having thus a finite stiffness. Therefore, the true behavior of a joint had to be accounted in the global analysis of the structure. This was achieved by using the moment-rotation curve, obtained from the determination of the mechanical properties of the joint in terms of its rotational stiffness (S_j), moment resistance ($M_{j,Rd}$) and rotational capacity (Φ_j).

The mechanical properties can be obtained from several models such as analytical, empirical, experimental, informational, mechanical and numerical ones. The most popular being the mechanical model, and among all of the ones available, the Component Method (a hybrid analytical-mechanical method), which will be described here. The Component Method, being the method recommended in the Eurocode 3, considers a joint as a set of individual basic components. Allowing the determination of the moment resistance and stiffness characteristics of the joint by calculating the ones of all the different components of it.

As mentioned in [19], the Eurocode provides information for evaluating the monotonic behavior of beam-to-column connections, but does not give any indication for the modeling of the cyclic behavior of the joint components.

In this paper, we will focus on the bolted stiffened extended end plate connections, and describe the Component Method procedure from [2] and described in [31] and [30] for this configuration.

4.2.1 Joint classification

Stiffness Classification

According to its rotational stiffness, a joint can be classified as rigid, nominally pinned or semi-rigid, by comparing its initial rotational stiffness $S_{j,ini}$ with the classifications boundaries shown in Figure 4.5. The limits are defined as functions of the stiffness of the beam and column.

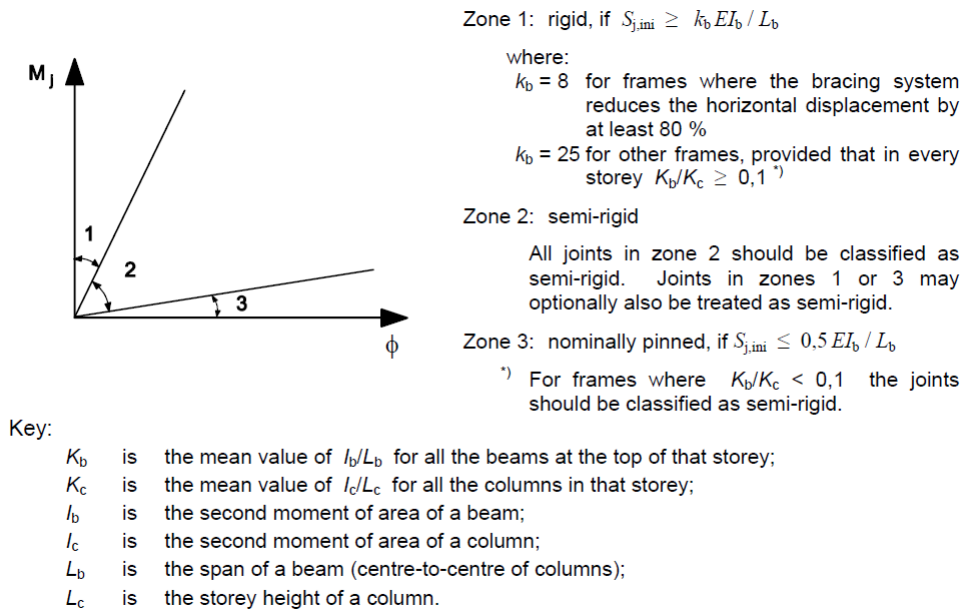


Figure 4.5: Classification of joints by stiffness, (*Chapter 5, [2]*)

Strength Classification

In terms of strength, comparing its design moment resistance $M_{j,Rd}$ with the resistance of the members that it connects (members adjacent to the joint), a joint can be classified as :

- Nominally pinned: The joint is capable of transmitting internal forces, without developing significant moments. A joint may be classified as pinned if its design moment resistance $M_{j,Rd}$ is not greater than a fourth of the design moment resistance for a full-strength joint (provided sufficient rotation capacity).
- Full strength joint: The joint must be able to develop a design moment resistant at least equal to the moment developed by its adjacent members, as described in Figure 4.6:
- Partial joint: Any joint that does not fall into the 2 other categories.

The eurocode specifies that if the effects of the behavior of the joints on the distribution of internal forces and moments within the structure are small, they

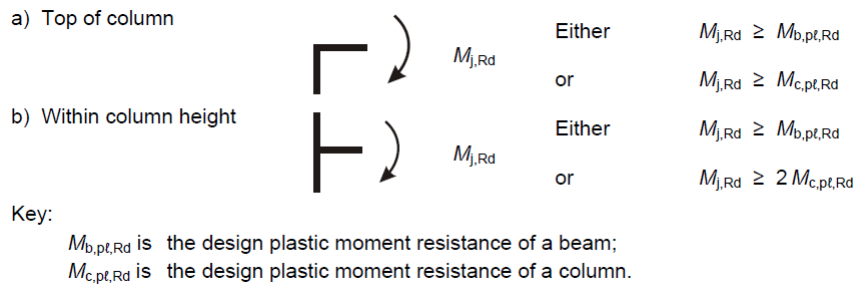


Figure 4.6: Full Strength Joint, (*Chapter 5, [2]*)

may be neglected. In order to know whether or not these effects can be neglected, 3 simplified joint models have to be distinguished:

- Simple: The joint is assumed not to transmit bending moments
- Continuous: The behavior of the joint is assumed to have no effect on the structure analysis
- Semi-continuous: The behavior of the joint needs to be accounted for in the analysis.

The type of joint model should be determined from Figure 4.7:

| Method of global analysis | Classification of joint | | |
|---------------------------|-------------------------|-------------------------|---|
| | Nominally pinned | Rigid | Semi-rigid |
| Elastic | Nominally pinned | Rigid | Semi-rigid |
| Rigid-Plastic | Nominally pinned | Full-strength | Partial-strength |
| Elastic-Plastic | Nominally pinned | Rigid and full-strength | Semi-rigid and partial-strength Semi-rigid and full-strength Rigid and partial-strength |
| Type of joint model | Simple | Continuous | Semi-continuous |

Figure 4.7: Type of Joint Model, (*Chapter 5, [2]*)

4.2.2 Resistance

We first have to identify the basic components localized in the different zones of the joint (Tension zone, shear zone, compression zone; see Figure 4.8).

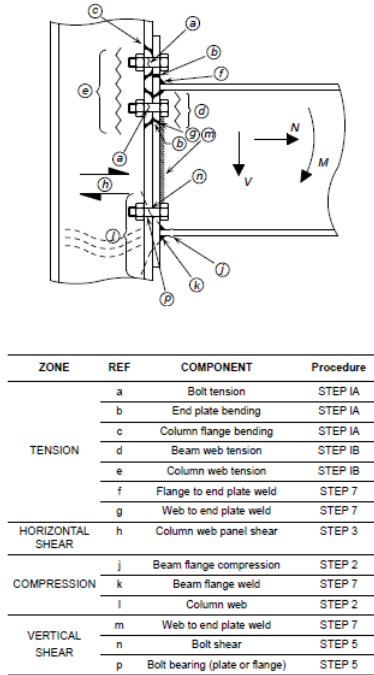


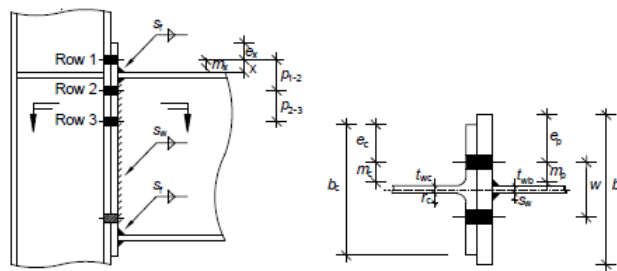
Figure 4.8: Joints components to be evaluated, (*Chapter 2, [30]*)

Then, we have to characterize the behavior of each component in terms of resistance-deformation. Finally, the components have to be assembled in a mechanical model that consists of springs and rigid elements which will result in one single equivalent element characterized by the joint moment-rotation relation.

In order to calculate the moment resistance of the joint, we will have to calculate the resistance of every component.

From Figure 4.8, we can see the different components present. In our configuration, the connection is doubled sided and submitted to equal but opposite moments. Thus the column web panel will be submitted to shear. The procedure will be the same, except that we will need to take it into account in the β coefficient (transformation parameter, see Figure 4.12).

The connection geometry must be specified, which is done in Figure 4.9



For the end plate:

$$m_p = \frac{w}{2} - \frac{t_{wb}}{2} - 0.8s$$

$$e_p = \frac{b_p}{2} - \frac{w}{2}$$

For the column flange:

$$m_c = \frac{w}{2} - \frac{t_{wc}}{2} - 0.8r_c$$

$$e_c = \frac{b_c}{2} - \frac{w}{2}$$

For the end plate extension only:

$$m_x = x - 0.8s_x$$

Adjacent to a flange or stiffener:

m_2 is calculated in a similar way to m_x , above. m_2 is the distance to the face of the flange or stiffener, less 0.8 of the weld leg length.

Note: dimensions m and e , used without subscripts, will commonly differ between column and beam sides

Figure 4.9: Connection Geometry, (*Chapter 2, [30]*)

Resistance zone

The resistance of the connection can then be summarized as in [30], as followed:

- Resistance of the bolt rows in tension:

The effective design tension resistance is equal to the least of the following resistance :

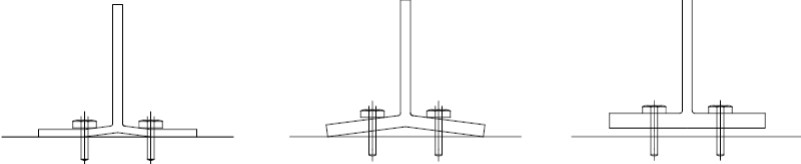
- End plate bending/bolt failure
- Column flange bending/bolt failure
- Column web in tension
- Beam web in tension

$$\mathbf{F}_{t,Rd(r)} = \min(\mathbf{F}_{t,fc,Rd}, \mathbf{F}_{t,wc,Rd}, \mathbf{F}_{t,ep,Rd}, \mathbf{F}_{t,wb,Rd}) \quad (4.16)$$

For the IPE600-HEB650 connection, we also have to account for the fact that the resistance of a group of several rows may be less than the sum of the resistances of the individual rows. For the IPE360-HEB340 and IPE450-HEB500, we only evaluate the resistance of individual rows because the bolts rows in tension are separated by the beam flanges.

To determine the potential tension resistance of the end-plate in bending and the column flange in bending, we need to calculate real yield line patterns converted into an equivalent T-stub. For that, we need to calculate the effective length of the equivalent T-stub according to table [T-Stub table].

The equivalent T-stub can have 3 failures modes:



| Mode 1 | Mode 2 | Mode 3 |
|--|---|--|
| The flange of the T-stub is the critical feature, and yields in double curvature bending | The flange of the T-stub yields and the bolts fail at the same load | The bolts are critical component and the resistance is the tension resistance of the bolts |

Figure 4.10: T-Stub Failure Modes, ([31])

Effective length of equivalent T-stub (column and flange)

| Bolt-row location | Bolt-row considered individually | | Bolt-row considered as part of a group of bolt-rows | |
|--------------------------------------|---|--|---|---|
| | Circular patterns $l_{eff,cp}$ | Non-circular patterns $l_{eff,nc}$ | Circular patterns $l_{eff,cp}$ | Non-circular patterns $l_{eff,nc}$ |
| Bolt-row adjacent to a stiffener | $2\pi m$ | αm | $\pi m + p$ | $0,5p + \alpha m - (2m + 0,625e)$ |
| Other inner bolt-row | $2\pi m$ | $4m + 1,25e$ | $2p$ | p |
| Other end bolt-row | The smaller of: $2\pi m$, $\pi m + 2e_1$ | The smaller of: $4m + 1,25e$, $2m + 0,625e + e_1$ | The smaller of: $\pi m + p$, $2e_1 + p$ | The smaller of: $2m + 0,625e + 0,5p$, $e_1 + 0,5p$ |
| End bolt-row adjacent to a stiffener | The smaller of: $2\pi m$, $\pi m + 2e_1$ | $e_1 + \alpha m - (2m + 0,625e)$ | Not relevant | Not relevant |

Figure 4.11: Length of Equivalent T-stub of a Stiffened Column Flange in Bending, ([31])

Where the value of α can be found in [2], Figure 6.11.

The resistance is thus equal to the minimum of the 3 modes:

- Mode 1 : $F_{T,1,Rd} = \frac{4M_{pl,1,Rd}}{m}$
- Mode 2 : $F_{T,2,Rd} = \frac{2M_{pl,2,Rd} + n \sum F_{t,Rd}}{m+n}$
- Mode 3 : $F_{T,3,Rd} = \sum F_{t,Rd}$

Where

$$M_{pl,1,Rd} = \frac{0.25 \sum l_{eff,1} t_f^2 f_y}{\gamma_{M0}}$$

$$M_{pl,2,Rd} = \frac{0.25 \sum l_{eff,2} t_f^2 f_y}{\gamma_{M0}}$$

$$n = e_{min} \leq 1.25m$$

$$F_{t,Rd} = \frac{0.9 f_{ub} A_s}{\gamma_{M2}}$$

$\sum F_{t,Rd}$ is the total of $F_{t,Rd}$ for all bolts in the T-stub

$$\gamma_{M2} = 1.25$$

$$\gamma_{M0} = 1.00$$

- The design resistance of a column web without stiffener in transverse tension is given by equation 4.2.2:

$$\mathbf{F}_{t,wc,Rd} = \frac{\omega \mathbf{b}_{eff,t,wc} \mathbf{t}_{wc} \mathbf{f}_{y,wc}}{\gamma_{M0}} \quad (4.17)$$

Where, as said earlier, the transformation parameter β is given in Figure 4.12:

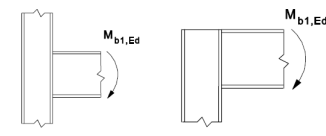
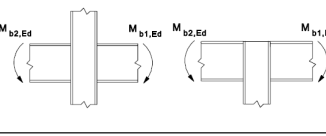
| Type of joint configuration | Action | Value of β |
|---|-----------------------------|-------------------|
|  | $M_{b1,Ed}$ | $\beta \approx 1$ |
|  | $M_{b1,Ed} = M_{b2,Ed}$ | $\beta = 0$ *) |
| | $M_{b1,Ed} / M_{b2,Ed} > 0$ | $\beta \approx 1$ |
| | $M_{b1,Ed} / M_{b2,Ed} < 0$ | $\beta \approx 2$ |
| | $M_{b1,Ed} + M_{b2,Ed} = 0$ | $\beta \approx 2$ |
| *) In this case the value of β is the exact value rather than an approximation. | | |

Figure 4.12: Transformation parameter β , (*Chapter 5,[2]*)

- The design resistance of a beam web in tension is given by equation 4.18:

$$F_{t,wb,Rd} = \frac{\omega b_{eff,t,wb} t_{wb} f_{y,wb}}{\gamma_{M0}} \quad (4.18)$$

Compression zone

The compression resistance is assumed to be provided entirely at the level of the bottom flange of the beam. For the beam, the resistance is assumed to be provided by the flange. On the column, we have to evaluate the length of the column web that resists the compression (it depends on the dispersion of the force through the end-plate and the column flange).

The design resistance in the compression zone is given by the minimum of the following:

- Column web in transverse compression
- Beam flange and web in compression

The design resistance of a column web in transverse compression is calculated by :

$$F_{c,wc,Rd} = \frac{\omega k_{wc} b_{eff,c,wc} t_{wb} f_{y,wc}}{\gamma_{M0}} \leq \frac{\omega k_{wc} \rho b_{eff,c,wc} t_{wb} f_{y,wc}}{\gamma_{M1}} \quad (4.19)$$

Where the effective width, shown in Figure 4.13 is given by:

$$\mathbf{b_{eff,c,wc} = t_{fb} + 2s_f + 5(t_{fc} + s) + s_p} \quad (4.20)$$

where:

$s = r_c$ for rolled I and H column sections

$s_f = \sqrt{2}a_p$

$s_p = 2t_p$ (provided that the dispersion line remains within the end plate)

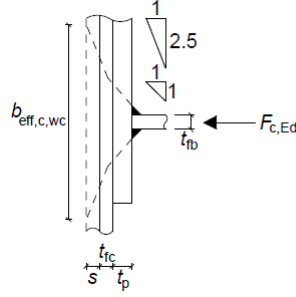


Figure 4.13: Effective Width β , ([30])

The reduction factor k_{wc} can be obtained from:

$$\theta_{com,Ed} \leq 0.7f_{y,wc} \rightarrow k_{wc} = 1$$

$$\theta_{com,Ed} > 0.7f_{y,wc} \rightarrow k_{wc} = 1.7 - \frac{\theta_{com,Ed}}{f_{y,wc}}$$

The reduction factor for plate buckling is obtained by:

$$\bar{\lambda}_p \leq 0.72 \rightarrow \rho = 1$$

$$\bar{\lambda}_p > 0.72 \rightarrow \rho = \frac{\bar{\lambda}_p - 0.2}{\bar{\lambda}_p}$$

Where

$$\bar{\lambda}_p = 0.932 \sqrt{\frac{b_{eff,c,wc} d_{wc} f_{y,wc}}{E t_{wc}^2}}$$

$$d_{wc} = h_c - 2(t_c + s)$$

The design resistance of a beam flange in compression is given by :

$$\mathbf{F_{c,fb,Rd} = \frac{M_{c,Rd}}{(h - t_{fb})}} \quad (4.21)$$

Shear zone:

In our cases, consisting of double-sided connections with moments from either side equal and opposite, the moment resistance of the connection may be limited by the column web panel.

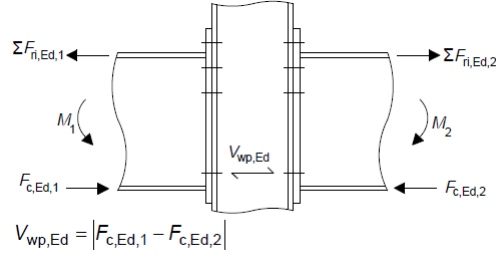


Figure 4.14: Shear forces in Column Web Panel, ([30])

The design resistance of a column web panel in shear is given by (for slenderness satisfying $d/t_w \leq 69\epsilon$) by:

$$\mathbf{V}_{wp,Rd} = \frac{0.9f_{y,wc}A_{vc}}{\sqrt{3}\gamma_{M0}} \quad (4.22)$$

Where:

$$A_{vc} = A_c - 2b_c t_{fc} - (t_{wc} - 2r_c)t_{fc} \text{ but } A_{vc} \leq \eta h_{wc} t_{wc}$$

$$\eta = 1$$

$$\epsilon = \sqrt{\frac{235}{f_{y,wc}}}$$

The Eurocode 1993-1-8 gives no indications for more slender webs. According to [30], it is suggested that 90% of the shear buckling resistance may be used:

$$\mathbf{V}_{wp,Rd} = 0.9\mathbf{V}_{bw,Rd} \quad (4.23)$$

Moment resistance determination:

The flexural resistance of the joint is obtained by summing the product between the tension forces and their respective lever arm (to the center of compression):

$$M_{c,Rd} = \sum F_{ri,Rd} h_i$$

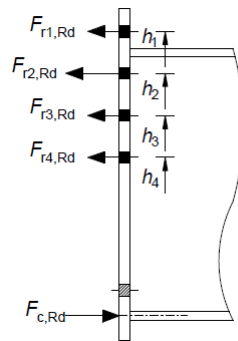


Figure 4.15: Tension and compression resistances contributing to moment resistance, ([30])

The sum of the tension forces has to be smaller than the compression resistance and the shear resistance. If it is not the case, an allocation of reduced bolt forces must be determined (see [30]) in order to account for the equilibrium.

Shear resistance of bolts

The resistance to vertical shear of the connection must also be verified. It is considered that in the Eurocode that the vertical shear is carried by the bolts present in the compression zone. The shear resistance is thus the smaller of the shear resistance of the bolt shank and the bearing resistance of the end-plate or column flange. If the bolts in the compression zone are not sufficient in order to carry the shear, it is necessary that bolts carrying tension also carry some shear. If the bolt has to resist combined tension and shear, an interaction criterion must be verified. However this criterion is quite difficult to evaluate due to the role of prying forces and it is conservatively assumed that the bolts in the tension zone can carry a resistance of maximum 28% of their design shear resistance.

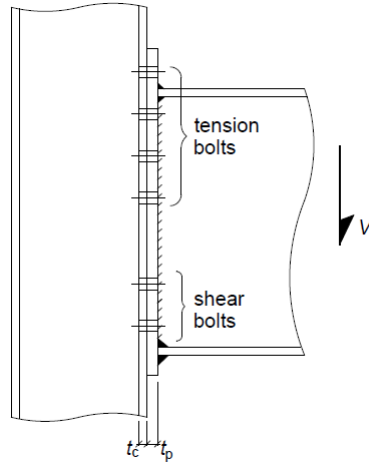


Figure 4.16: Tension and shear bolts, ([30])

The shear resistance is thus calculated by:

$$\mathbf{F}_{v,Rd} = \frac{\alpha_v \mathbf{f}_{ub} \mathbf{A}_s}{\gamma_{M2}} \quad (4.24)$$

$\alpha_v = 0.5$ for 10.9 bolts ; $\alpha_v = 0.6$ for 8.8 bolts

- The bearing resistance, which is equal to the smaller of the bearing resistance of the end-plate and the column flange, both given by:

$$\mathbf{F}_{b,Rd} = \frac{k_1 \alpha_b \mathbf{f}_u \mathbf{d}_B \mathbf{t}}{\gamma_{M2}} \quad (4.25)$$

$$k_1 = \min(2.8 \frac{e_2}{d_0} - 1.7; 2.5)$$

$$\alpha_b = \min(\alpha_d; \frac{f_u b}{f_u}; 1.0)$$

$t = t_p; t_{fc}$ depending if calculated for end-plate or column flange

$$\alpha_d = \frac{e_1}{3d_0} \text{ for end bolts}$$

$$\alpha_d = \frac{p_1}{3d_0} - \frac{1}{4} \text{ for end bolts}$$

4.2.3 Stiffness

As explained before, a joint can be rigid, semi-rigid or pinned. We defined the classification boundaries before. In order to classify a joint, its initial rotational stiffness has to be calculated according to [2]. The following spring model for the multi-rows end-plate joint is considered:

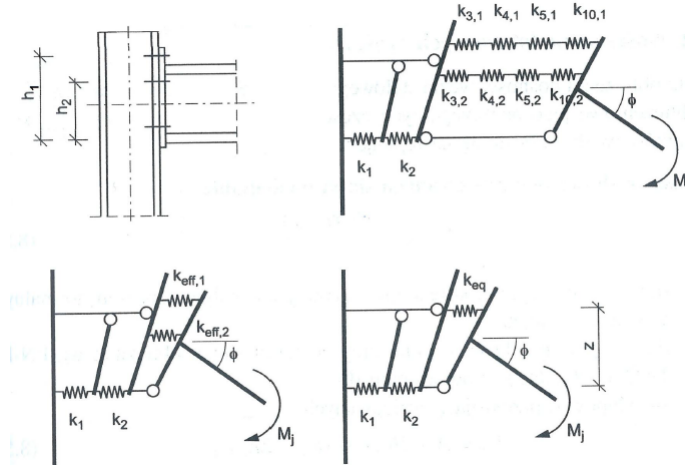


Figure 4.17: Spring model for multi bolt-rows end-plate joints, ([31])

This spring model allows us to calculate the initial rotational stiffness by:

$$\mathbf{S}_{j,ini} = \frac{Ez^2}{1/k_1 + 1/k_2 + 1/k_{eq}} \quad (4.26)$$

Where

$$k_{eq} = \frac{\sum_r k_{eff,r} h_r}{z_{eq}}$$

$$k_{eff,r} = \frac{1}{\sum_i k_{i,r}}$$

$$z_{eq} = \frac{\sum_r k_{eff,r} h_r^2}{\sum_r k_{eff,r} h_r} \text{ is the equivalent lever arm}$$

Determination of the k coefficient of every component:

- Column web panel in shear:

Unstiffened : $k_1 = \frac{0.38A_{vc}}{\beta_z}$

Stiffened : $k_1 = \infty$

Where

$\beta = 2$ in our case

- Column web in compression:

Unstiffened : $k_2 = \frac{0.7b_{eff,c,wc}t_{wc}}{d_c}$

Stiffened : $k_2 = \infty$

In case of bolted extended end-plate connection, the equivalent stiffness coefficient k_{eq} is based on the following k_i coefficient:

- Column web in tension

Unstiffened : $k_3 = \frac{0.7b_{eff,t,wc}t_{wc}}{d_c}$

Stiffened : $k_3 = \infty$

- Column flange in bending (for a single bolt-row in tension)

$$k_4 = \frac{0.9l_{eff}t_{fc}^3}{m^3}$$

Where

m is given in EN 1993-1-8 §6.2.6.4 Figure 6.8

- End-plate in bending (for a single bolt-row in tension)

$$k_5 = \frac{0.9l_{eff}t_p^3}{m^3}$$

Where

m is given in EN 1993-1-8 §6.2.6.5 Figures 6.10

- Bolts in tension (for a single bolt-row in tension)

Unstiffened : $k_{10} = \frac{1.6A_s}{L_b}$

Stiffeners

There are many ways to increase the resistance and the rigidity of our connection with the use of stiffeners.

Rib

First of all, we have to consider the rib stiffener.

Indeed, the rib stiffener is not yet covered by the Eurocode. We will thus use the method proposed in [29]

As explained in [28], based on the work of [29], after many experimental and numerical results comparisons, it has been considered as the best solution to design the rib is based on a strut model. The angle of the strut being assumed equal to the rib diagonal angle. See the principal stress plot in Figure 4.18:

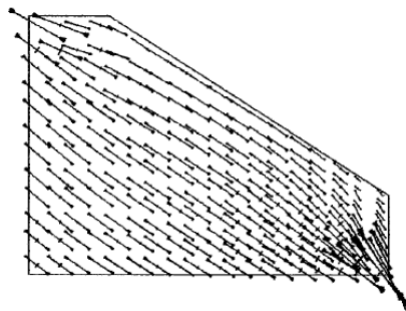


Figure 4.18: Principal stress distribution in the rib, ([29])

It was proven that the length of the rib does not have a large influence, and considering the width and the height as practical ranges, the minimum thickness can be calculated by considering the Von Mises yielding criterion and using the interaction forces N and Q as followed:

$$\mathbf{t} \geq \frac{\sqrt{\mathbf{Q}^2 + 3\mathbf{N}^2}}{\mathbf{b}(\Phi\mathbf{F}_{\mathbf{yr}})} \quad (4.27)$$

Where

$$Q = \frac{\left(\frac{(0.21a+0.15L')ad_b}{I_b}\right)}{(1/\eta)\frac{0.6\sqrt{a^2+b^2}\sqrt{(a-c)^2+(b-c)^2}}{(ab-c^2)t} + \frac{(0.18b+0.30d_b)ad_b}{I_b}} * V_p l$$

$$N' = \left(\frac{b}{a}\right) * Q$$

Where

a,b,c are the dimension of the rib as seen in Figure [29]

$\Phi = 0.90$

$\eta = 1.5$; gives good results according to [29]

L' is the span of the beam between the rib tips

We also have to take into account the stiffness of the rib, which can be calculate assuming the strut of Figure 4.19 by:

$$k_e = \frac{A_e E}{L_e} = \frac{\eta(ab - c^2)tE}{0.6\sqrt{a^2 + b^2}\sqrt{(a - c)^2 + (b - c)^2}} \quad (4.28)$$

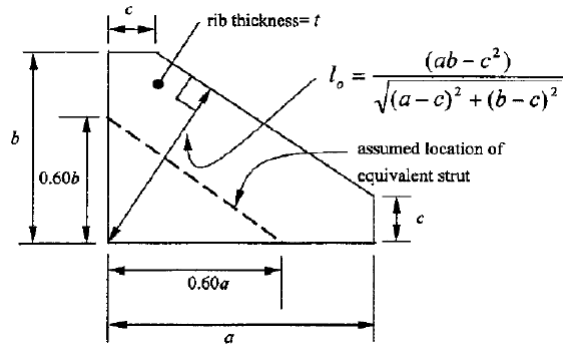


Figure 4.19: Definition of rib cross section, ([29])

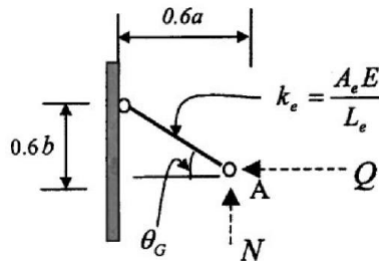


Figure 4.20: Equivalent stress model, ([29])

Continuity Plate

As seen earlier, the presence of continuity plate in the tension and the compression zone of the column web panel plays a big role in the stiffness value of these components.

They also increase the bending resistance of the column flange and the tension resistance of the column web in the tension zone. As well as increasing the compression resistance of the column web in the compression zone.

In our case, the continuity plates are all full depth and are present symmetrically on both side of the column web. They are aligned with the corresponding beam flange.

According to [2], when continuity plate are used in both compression and tension zone, the design plastic shear resistance of the column web panel $V_{wp,Rd}$ may be increased by $V_{wp,add,Rd}$, given by:

$$V_{wp,add,Rd} = \frac{4M_{pl,fc,Rd}}{d_s} \text{ but } V_{wp,add,Rd} \leq \frac{2M_{pl,fc,Rd} + 2M_{pl,st,Rd}}{d_s} \quad (4.29)$$

Supplementary web plate (SWP):

Supplementary web plate will increase the shear resistance of the web panel, and also have an increasing effect on the tension and compression resistance of the column web panel.

Supplementary web plates are also used to increase the rotational stiffness of a joint by increasing the stiffness of the column web in shear, compression or tension.

According to the Eurocode 1933-1-8, the supplementary web plate must fulfill the following requirements:

- The steel grade of the SWP should be the same as the one of the column.
- The thickness of the SWP should be at least equal to the thickness of the column web.
- The width of the SWP should go from the fillets of the column of one flange to the ones of the other flange.
- The width should not exceed $40\epsilon t_s$.
- The length of the SWP should at least go from the limit of the tension zone to the limit of the compression zone on the column web.

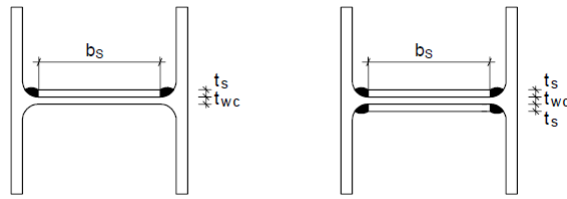


Figure 4.21: Supplementary web plate, (*Chapter 6, [2]*)

If the previous requirements are respected, the Eurocode considers that supplementary web plate (in the case of full penetration welds):

- Increase the web compression resistance by 50% with a plate on one side and by 100% with plates on both sides ($\rightarrow t_{w,eff} = 1.5t_{wc}$ for one plate and $t_{w,eff} = 1.5t_{wc}$ for 2 plates)
- Increase the web tension resistance by 50% with a plate on one side and by 100% with plates on both sides. ($\rightarrow t_{w,eff} = 1.5t_{wc}$ for one plate and $t_{w,eff} = 1.5t_{wc}$ for 2 plates)
- Increase the web panel shear resistance by 75% with a plate on one side. Indeed, according to the Eurocode, a second plate does not increase the shear resistance of the column web panel. (\rightarrow shear area is increased by $b_s t_{wc}$.)

Chapter 5

FE Validation

Having a better understanding of the behavior of the joints is fundamental. Therefore, the most reliable sources of information are the experimental studies. However, these studies are very expensive to carry. Indeed, in order to account for the large variability of the parameters, and their influence on the joint, a large number of analysis have to be carried out.

In order to do so, models using the finite elements method can be used. These models are inexpensive and robust, they allow the understanding of local effects which are difficult to measure accurately physically and they can be used to generate extensive parametric studies.

Thus, the finite element models used in this project, were done using the software ABAQUS v.6-13. We will present here after the basic modeling assumptions and the validation against experimental tests given by literature of the models used, as described in [33], on which our models are based on.

Two specimens out of the five stiffened extended end plate connections with different end-plate thickness from [25] were selected to be numerically modeled in order to validate the FE inputs used in the models.

Although, the models that we carried out (two sided beam connection) are not exactly similar as the one presented here (one sided beam connection) , the validation presented here is relevant to our study.

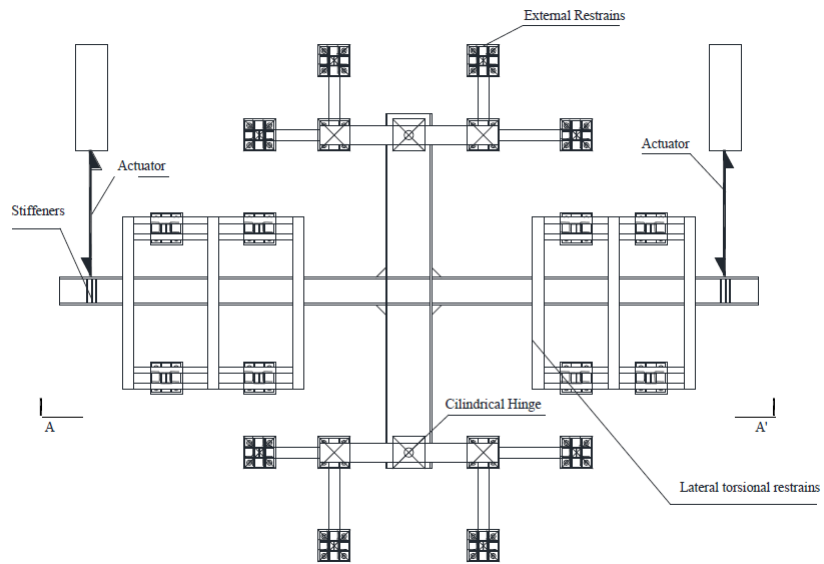


Figure 5.1: Details of the setup), ([25])

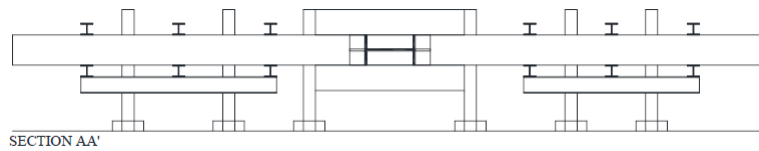


Figure 5.2: Section AA' of setup, ([28])

5.1 Model Assumption

5.1.1 Model Geometry

The beam and column length considered in the ABAQUS model are up to the point where the physical restraints are placed on the experimental specimens (as in Figure 5.1 and 5.2). The additional plate stiffener welded at the end of the beam (used to increase the stiffness of the beam section where the load is applied by means of the actuator) and at the end of the column (where the external hinge supports are located) are not represented in the FE model because they are considered to have a negligible influence on the behavior of the joint.

5.1.2 Units

There is no unit system in ABAQUS. Therefore, a consistent set of units has to be applied by the user. This is extremely important in order to avoid basic problems caused by an inconsistent set of units. The units used to input data in ABAQUS are shown in Table 5.1

Table 5.1: Units for ABAQUS

| | Length | Force | Stress | Density | Elastic Modulus |
|------|--------|-------|------------------|-------------|------------------|
| Unit | mm | N | MPa [N/mm^2] | Ton/ mm^3 | MPa [N/mm^2] |

5.1.3 Element type

The finite element type C3D8I is used to represent the steel beams, columns and high strength bolts. It consists of an 8-node linear brick with incompatible mode. This element has 13 additional degrees of freedom [7], and it is conceived to eliminate the so-called parasitic shear stresses that are observed in problems where bending is dominant. They are used because they can effectively avoid the shear locking phenomenon, which could have a significant effect on the initial stiffness of the connection.

5.1.4 Interaction

Three different types of interactions were used in the models, they are presented hereafter:

- Tie constraint : This type of interaction ties two separate surfaces together such that no relative displacement is allowed between them. It is used to represent the full penetration weld behavior, which is applied to the connections

between the beam and the end-plate, between the rib and the end-plate, between the continuity plates and the column, and between the supplementary web plates and the column.

- **Rigid-Body Constraint** : This type of interaction is used to simulate the planar behavior of a cross section and to integrate the mechanical response of the whole section. Indeed, with this type of constraints, it is possible to apply the boundary conditions of the whole section in one point called a reference point (which has to be defined). See Figure 5.7.
- **Contact interaction**: This type of interaction is used in order to represent the interaction between surfaces that cannot penetrate each other and that are characterized by friction sliding (Surfaces of the bolt shank and hole, surface of the bolt head and the corresponding column flange surface, surface of the bolt nut and the corresponding end-plate surface, the surface in contact between the end-plate and the column). In order to do so, the tangential behavior is described by a "Coulomb friction" having a friction coefficient equal to 0.4. The normal behavior is described by "Hard contact".

5.1.5 Material Property

In order to have the most accurate results possible, the material stress-strain curve from the experimental tests used should be accounted for. However, since there is a lack of data from the experimental tests, other materials tests reported in literature were used for the stress-strain curve. As mentioned in [33], the plasticity model implemented in ABAQUS is based on Chaboche model and consists of a nonlinear kinematic hardening component and an isotropic hardening component, as described by Wang et al. (2013).

Plates and members properties

For all elements (members and plates) of the connection, the same global material property of Steel (S355) is used. The Young's Modulus is assumed to be equal to 210000 MPa and the Poisson's ratio is assumed to be equal to 0.3..As shown in the plastic true stress - true strain is in Figure 5.3, the yield strength is 443.75 MPa and ultimate strength is 752.19 MPa.

Bolts Properties

Three different diameters of high strength bolts were used : M27, M30, M36. They are all of grade 10.9. The plastic true stress-true strain of the bolt material is shown in figure 2.2:

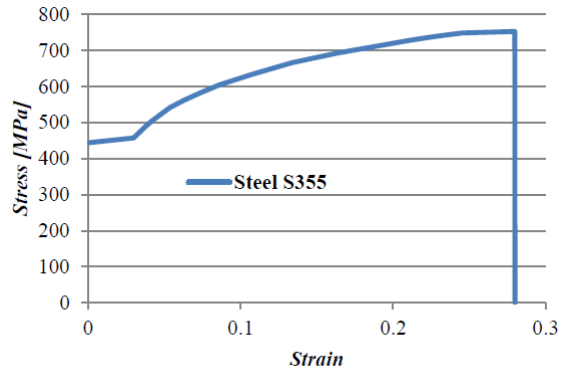


Figure 5.3: Plastic stress - strain diagram for S355, ([33])

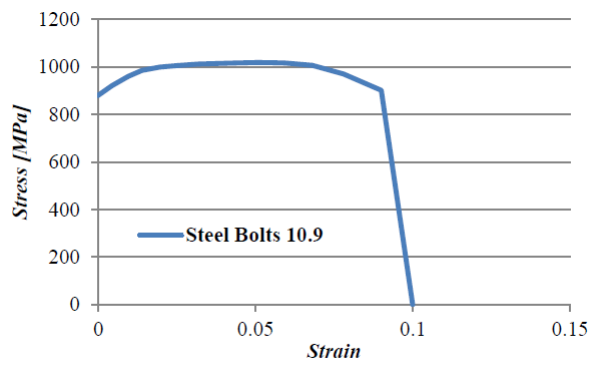


Figure 5.4: Plastic stress - strain diagram for Bolts 10.9, ([33])

Some considerations have to be made for the modeling of the bolts. Indeed, the bolt shank is modeled by meshing a solid cylinder having the nominal circular gross area of the bolt. But since the bolt shank strength is governed by the threaded part, which has an effective bolt area smaller than the nominal gross area, the material stress has to be scaled in order to simulate the bolt strength using the nominal shank area. It is done with equation 5.1:

$$f_{\text{effective}} = f_{\text{actual}} \frac{A_{\text{effective}}}{A_{\text{gross}}} \quad (5.1)$$

Moreover, the threaded part of the bolt also affects the elastic stiffness of the shank. The bolt stiffness can be obtained from [Swanson and Leon (2001)] by :

$$\frac{1}{k_b} = \frac{f d_b}{A_B E} \frac{L_s}{A_B E} \frac{L_{tg}}{A_{Be} E} \frac{f d_B}{A_{Be} E} \quad (5.2)$$

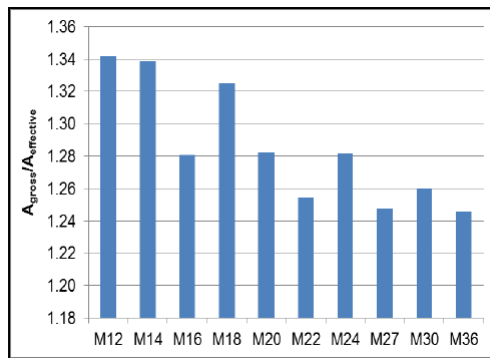


Figure 5.5: Difference between nominal and net area of several bolt types, ([33])

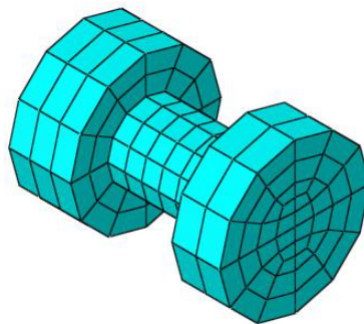


Figure 5.6: Meshed Bolt, ([33])

Step Setting

The analysis carried out is a Dynamic Implicit one. It is realized in two steps in order to account for two different loading histories, both of them having their own amplitude. In the first step, consisting of a 1000 seconds time interval, the clamping is applied to the bolts. In the second step, a 71500 seconds time interval, a monotonic loading with final displacements of 500 mm, having opposite directions, is applied on the end of both beams. The "Quasi-Static" load application method is used and the non linear effects of large displacement are included.

Boundary Conditions and Loads

The boundaries conditions are applied to the models in order to represent the restrictions of the test setup. They are simulated by means of special nodes in the models (Reference Points). Thus the following boundary conditions are considered:

- The both ends of the column are pinned, i.e. they have all the translational degrees of freedom and the rotation around the axis of the column blocked.
- Constraints that avoid lateral torsional buckling of the beams, i.e. rotation around the beam axis and the lateral out of plane displacement of the section are modeled. 2 of these constraints are placed at 1000 meters of distances from each other starting 1000 meters from the ends of both beams. See Figure 5.7

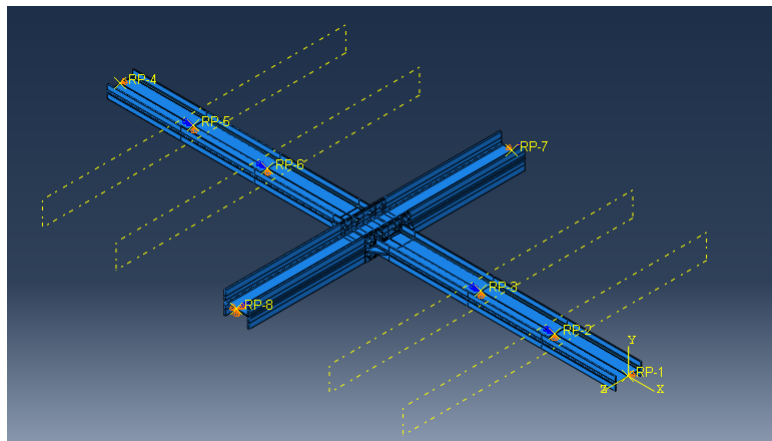


Figure 5.7: ABAQUS Model (For the current project)

- A displacement history consistent with the experimental loading applied by the actuator is imposed on the end of both beams (same value, opposite

direction). In the initial phase the displacement is restrained and in the second, it varies according to the imposed loading protocol. This allows to have a smooth increase in the bending moment.

We have to give a high importance in the pretensioned force applied to the bolts, since it has a large impact on the seismic behavior of the the connection. In ABAQUS, the "Bolt Force" option was used to apply the pretension load in the middle of the bolt section (the value of the pretension depends on the diameter of the bolt). The law of variation of the clamping loading increases linearly up to 100 seconds and then keeps the force constant. The design value of the pretension force was calculated according to the EUROCODE [2]. The applied load and the effect of clamping on the End Plate is shown in Figure 5.8 :

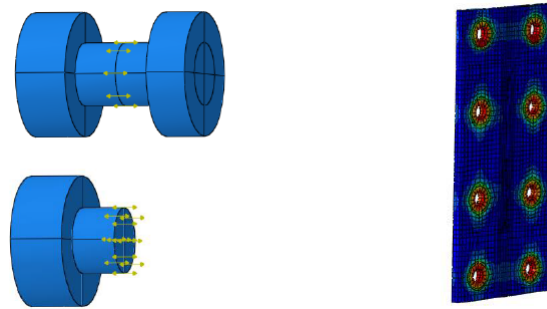


Figure 5.8: Bolt load definition and the effect of Clamping on the End Plate, [33]

Output from ABAQUS

Once the ABAQUS analysis is completed, several parameters have to be extracted from the output files such as the "z" displacement in the load direction of the reference points at the extremity of the beams, the reaction force in the same points (which is used to calculate the moment applied to the connection through time, considering the lever arm of the point relative to the center of the connection), the "x" displacement of the continuity plates (above and below), the "x" and "z" displacements of the the tip of the rib on the beam flanges, the horizontal reactions of the top and bottom of the column, the bolts reactions,... An important output was the PEEQ results. It represents the equivalent plastic strain, which is defined in [32].

Finally, the moment-rotation curve of the connection has to be found.

5.2 Validation of the FE assumptions

Although our joint is not exactly similar to the one tested in [25], i.e. the joint presented in this paper is double sided while the joint tested was one sided, the connection configuration is the same : it is based on standard stiffened end-plate moment connection for multi-storey buildings with the end-plate extending on both sides, the column flange and end-plate are stiffened by ribs, the thickness of the continuity plates and the ribs are at least equal to the thickness of the flange and the web of the beam, the thickness of the column flange is equal to the thickness of the end-plate in the connection zone. We can see hereafter the details of the setup and specimen geometry tested in [25], as well as the connection dimensions here after:

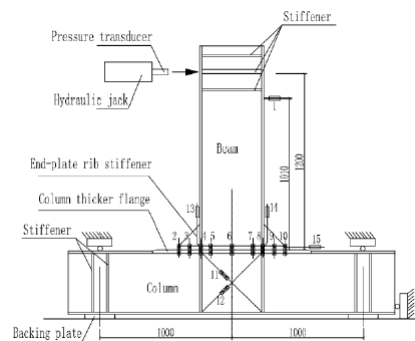


Figure 5.9: Test Specimen and loading arrangement, [25]

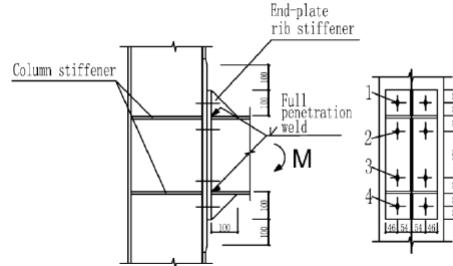


Figure 5.10: Details of connection, [25]

| Dimension | Beam | | Column | | Stiffeners | | CASE 1 | | CASE 2 | |
|-----------|--------|------|--------|------|------------|-----|--------|-------|--------|-------|
| | Flange | Web | Flange | Web | Rib | CP | EP | Bolts | EP | Bolts |
| t [mm] | 12 | 8 | 12 | 8 | 10 | 12 | 20 | M24 | 16 | M20 |
| b [mm] | 200 | 276 | 250 | 276 | 100 | 121 | 200 | | 200 | |
| h [mm] | 1200 | 1200 | 2000 | 2000 | 100 | 276 | 500 | | 500 | |

Figure 5.11: Detailed dimensions of the connection, [25]

We can thus make the reasonable assumption that the validation of the FE method for this one-sided configuration will assure the validation of the double-sided beam connection presented in this paper.

In order to define the plastic behavior for all material, the measured yield and tensile strength are used to define the plastic behavior for all materials. The material properties obtained from the experimental tests are presented here:

| Material | Measured yield strength (MPa) | Measured tensile strength (MPa) | Measured elastic modulus (MPa) | Design value of bolt pre-tension force (kN) | Measured bolt average pre-tension force (kN) |
|--------------------------------|-------------------------------|---------------------------------|--------------------------------|---|--|
| Steel (thickness \leq 16 mm) | 391 | 559 | 190 707 | – | – |
| Steel (thickness $>$ 16 mm) | 363 | 537 | 204 228 | – | – |
| Bolts (M20) | 995 | 1160 | – | 155 | 185 |
| Bolts (M24) | 975 | 1188 | – | 225 | 251 |

Figure 5.12: Material Properties, [25]

5.2.1 Result Comparison

A comparison between the experimental results and the FE results was carried out in [33] on 2 specimens tested in [25].

Case 1 ($t_{ep} = 20mm$ and $d_b = 24mm$)

The FE method shows very good results in comparison with the experimental results, as can be seen in the following figures. Indeed, it can be observed that for both methods the failure mode is the same (buckling of beam flange and web in compression) and a good matching of the Moment-Rotation Curves.

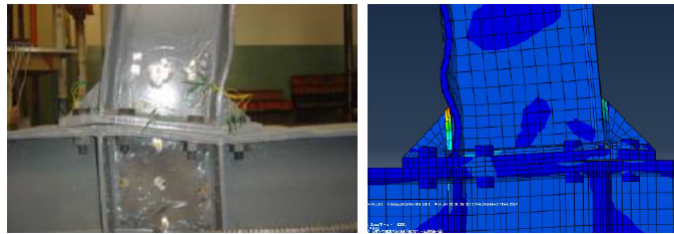


Figure 5.13: Failure mode comparison between experimental and FEA (Case 1), Experimental : [25] , FEA : [33]

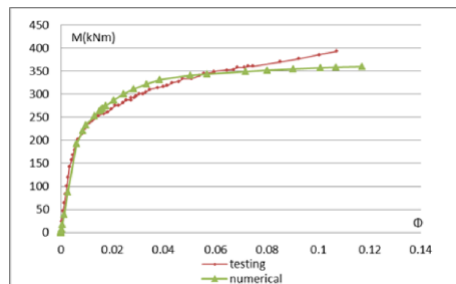


Figure 5.14: Moment-rotation curve comparison (Case 1), [25]

Case 2 ($t_{ep} = 16mm$ and $d_b = 20mm$)

The FE method shows very good results in comparison with the experimental results, as can be seen in the following figures. Indeed, it can be observed that for both methods the failure mode is the same (bolt fracture and buckling of end plate rib stiffener in compression) and good matching in terms of moment resistance and rotational capacity.

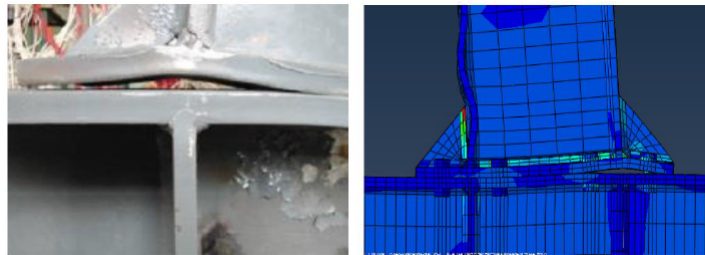


Figure 5.15: Failure mode comparison between experimental and FEA (Case 2), Experimental : [25] , FEA : [33]

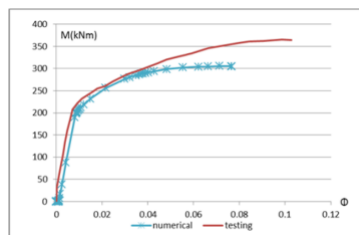


Figure 5.16: Moment-rotation curve comparison (Case 2), [25]

Chapter 6

Parametric Study

6.1 Geometry

As mentioned earlier, this paper will be focused on the investigation of the behavior of the panel zone of the column.

A parametric study was conducted with the FE program ABAQUS.

The joint configurations (all are double sided) that are investigated are the following:

- IPE360-HEB340 (equal and partial)
- IPE450-HEB500 (equal and partial)
- IPE600-HEB650 (equal and partial)

The design of these joints has been done according to the procedure followed in the EQUALJOINT project.

The dimensions of the different connections are presented hereafter:

Table 6.1: Equal Strength

| Beam | | Column | | End-Plate | | | Ribs | | | | Bolts | | | | | | |
|---------|------------|---------|------------|-----------|------|------|------|----------|--------------|------|-------|------|------|-------|--------|---------|-------|
| Section | Length | Section | Length | h | b | t | h | α | b | t | d | e | w | p_1 | p'_1 | p''_1 | p_2 |
| [-] | [mm^2] | [-] | [mm^2] | [mm] | [mm] | [mm] | [mm] | [mm] | [$^\circ$] | [mm] | [mm] | [mm] | [mm] | [mm] | [mm] | [mm] | [mm] |
| IPE360 | 3260 | HEB340 | 3745 | 600 | 280 | 18 | 120 | 30 | 140 | 20 | 27 | 50 | 60 | 160 | 180 | - | 160 |
| IPE450 | 3223 | HEB500 | 3745 | 770 | 300 | 20 | 160 | 30 | 190 | 20 | 30 | 55 | 70 | 200 | 260 | - | 160 |
| IPE600 | 3150 | HEB650 | 3745 | 1100 | 300 | 22 | 250 | 30 | 295 | 20 | 33 | 55 | 70 | 95 | 210 | 380 | 160 |

An equal strength connection means that the plastic moment resistance of the connection is equal to the plastic flexural resistance of the adjacent beam.

Table 6.2: Partial Strength

| Beam | | Column | | End-Plate | | | Ribs | | | | Bolts | | | | | | |
|---------|------------|---------|------------|-----------|------|------|------|----------|--------------|------|-------|------|------|-------|--------|---------|-------|
| Section | Length | Section | Length | h | b | t | h | α | b | t | d | e | w | p_1 | p'_1 | p''_1 | p_2 |
| [-] | [mm^2] | [-] | [mm^2] | [mm] | [mm] | [mm] | [mm] | [mm] | [$^\circ$] | [mm] | [mm] | [mm] | [mm] | [mm] | [mm] | [mm] | [mm] |
| IPE360 | 3260 | HEB340 | 3745 | 600 | 280 | 16 | 120 | 30 | 140 | 20 | 27 | 50 | 60 | 160 | 180 | - | 160 |
| IPE450 | 3223 | HEB500 | 3745 | 770 | 300 | 18 | 160 | 30 | 190 | 20 | 30 | 55 | 70 | 200 | 260 | - | 160 |
| IPE600 | 3150 | HEB650 | 3745 | 1100 | 300 | 20 | 250 | 30 | 295 | 20 | 33 | 55 | 70 | 95 | 210 | 380 | 160 |

On the other side, a partial strength resistance means that the plastic moment resistance of the connection is lower than the plastic flexural resistance of the adjacent beam. In our case, the partial strength connection differs from the equal one only in the thickness of the end-plate. For the Partial Strength joint, the joint capacity was considered to be 80% of the beam resistance.

6.2 Web Panel Stiffeners Investigation

For every joint, we will study the influence of reinforcements on the column web panel zone:

- Supplementary web plate ($b = 534$ mm, $L = 1100$ mm) which cover the entire column web, until the root fillet of the column profile will be added (according to the European and to the American specifications) in order to strengthen the column web panel zone . Indeed, as seen earlier, for interior joints submitted to antisymmetric loading, the CWP in shear can be the weakest component and create big displacement due to its very ductile behavior. As explained in [9], a balanced design in order to share the plastic demand between the column web panel in shear and the beam in bending is encouraged, allowing for a smaller plastic rotation demand on the beam compared to the strong panel-weak beam solution. Therefore, connections with different SWP configuration and geometry will be tested in order to overstrengthen the panel zone so that its shear resistance is big enough for the beam to be in the inelastic range. Basically, when the panel zone is not strengthened (or with SWP not thick enough to develop the flexural resistance of the beam), the beam will not be in plastic deformation (or a little bit). On the contrary, when the strengthening is consequent, the beam will be in plastic deformation. In this case, the contribution of the shear deformation of the CWP in the total deformation of the connection will not be as important (smaller contribution with stronger SWP).

The difference in the American specifications is just that the SWP are fixed on the edge of the column flanges (We will represent them without CP)

FE models realized:

Table 6.3: IPE 360 Equal Strength

| $M_{wp}/M_{pl,b,rd}$ | Number of SWP | Thickness of SWP | AISC |
|----------------------|---------------|------------------|------|
| 1.25 | 2 | 13 | ✓ |
| 1 | 2 | 8 | ✓ |
| 0.75 | 1 | 6 | - |
| 0.5 | 0 | - | - |

Table 6.4: IPE 360 Partial Strength

| $M_{wp}/M_{pl,b,rd}$ | Number of SWP | Thickness of SWP | AISC |
|----------------------|--------------------------|------------------|------|
| 1.25 | 2 | 8 | ✓ |
| 1 | 1 | 9 | ✓ |
| 0.75 | 0 | - | - |
| 0.5 | MNE (Model non existent) | MNE | MNE |

Table 6.5: IPE 450 Equal Strength

| $M_{wp}/M_{pl,b,rd}$ | Number of SWP | Thickness of SWP | AISC |
|----------------------|---------------|------------------|------|
| 1.25 | 2 | 9 | ✓ |
| 1 | 1 | 10 | ✓ |
| 0.75 | 0 | - | - |
| 0.5 | MNE | MNE | MNE |

Table 6.6: IPE 450 Partial Strength

| $M_{wp}/M_{pl,b,rd}$ | Number of SWP | Thickness of SWP | AISC |
|----------------------|---------------|------------------|------|
| 1.25 | 1 | 10 | ✓ |
| 1 | 1 | 5 | ✓ |
| 0.75 | 0 | - | - |
| 0.5 | MNE | MNE | MNE |

Table 6.7: IPE 600 Equal Strength

| $M_{wp}/M_{pl,b,rd}$ | Number of SWP | Thickness of SWP | AISC |
|----------------------|---------------|------------------|------|
| 1.25 | 2 | 7 | ✓ |
| 1 | 1 | 7 | ✓ |
| 0.75 | 0 | - | - |
| 0.5 | MNE | MNE | MNE |

Table 6.8: IPE 600 Partial Strength

| $M_{wp}/M_{pl,b,rd}$ | Number of SWP | Thickness of SWP | AISC |
|----------------------|---------------|------------------|------|
| 1.25 | 1 | 15 | ✓ |
| 1 | 1 | 7 | ✓ |
| 0.75 | 0 | - | - |
| 0.5 | MNE | MNE | MNE |

We thus have 31 different configurations (including 12 American and 19 European).

- For all different SWP configurations here above, in addition to the model without continuity plate (CP), models with CP of thickness equal to respectively 0.5, 1 and 1.5 the thickness of the beam flange will be added (Except for the AISC configuration, which are only tested without CP). Which gives us a total of 88 models to be tested numerically.

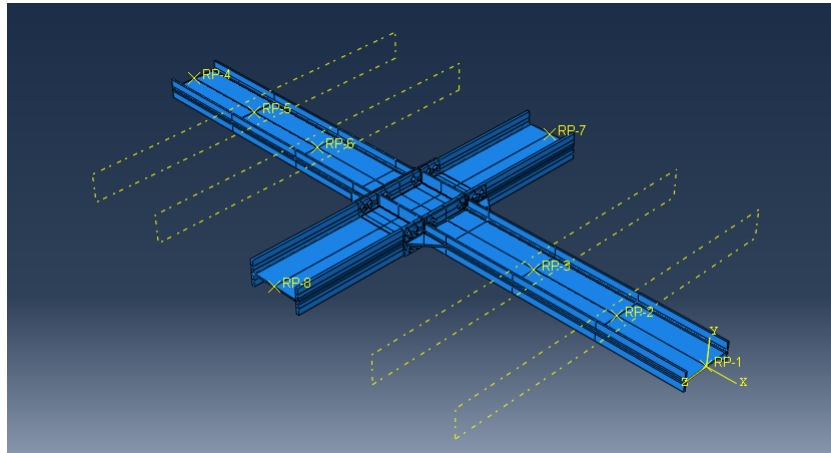


Figure 6.1: Example of FE Model (IPE600-HEB650 with CP and SWP.), (*Abaqus*)

The FE program abaqus will not give us directly the moment-rotation curves that we are interested in. Indeed, the value that can be obtained from ABAQUS are the reaction at the end of the beam and the displacement at the same point. Thus knowing the lever arm, we can calculate the value of the moment and the rotation at the middle of the column.

Despite the goal of the study to be the investigation of the behavior of beam-

to-column joints in seismic areas, our analysis were done under monotonic loading instead of a cyclic loading. We will thus obtain a monotonic curve which can give us a good prediction of the envelope of the cyclic curve. Furthermore, it shortens the time of the analysis and facilitates the material properties, which is quite useful for such a short time study.

Unfortunately, although many models were created, only very few gave results. Indeed, most of the models did not converge. This divergence is most likely related to the quality of the mesh, and to some imperfections in the geometry. These small imperfections can have a huge influence on the convergence of the numerical analysis when the plastic demand and the displacement are big (Which is the case when the column web panel zone has the biggest contribution in the total deformation of the connection).

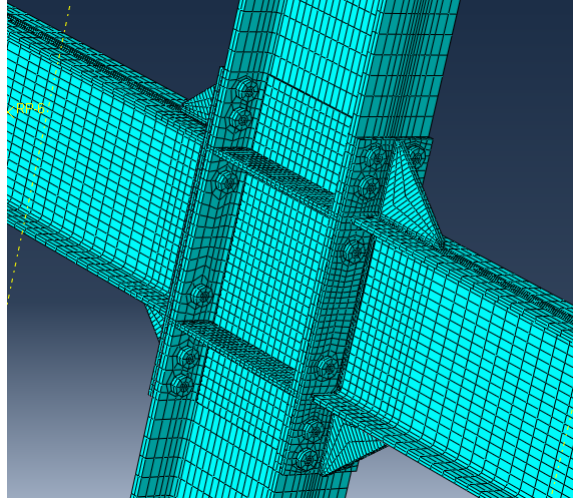


Figure 6.2: Meshing detail of a model (IPE600-HEB650 with CP and SWP.), (*Abaqus*)

Thus, the models that gave us results are the following :

- Model (a) IPE600-HEB650 with 2 SWP of 7 mm ($M_{wp}/M_{pl,b,rd} = 1.25$): 4 configurations of CP (No CP, $t_{CP} = 0.5t_{bf}$, $t_{CP} = t_{bf}$, $t_{CP} = 1.5t_{bf}$)
- Model (b) IPE600-HEB650 with 1 SWP of 7 mm ($M_{wp}/M_{pl,b,rd} = 1$): 4 configurations of CP (No CP, $t_{CP} = 0.5t_{bf}$, $t_{CP} = t_{bf}$, $t_{CP} = 1.5t_{bf}$)

Before even comparing the different configurations, the loading being equal but in opposite direction on the end of both beams, we have to check if the results on

both sides of the connection are similar. We can see from Figure 6.3 and 6.4 that it is the case for our 2 different configurations:

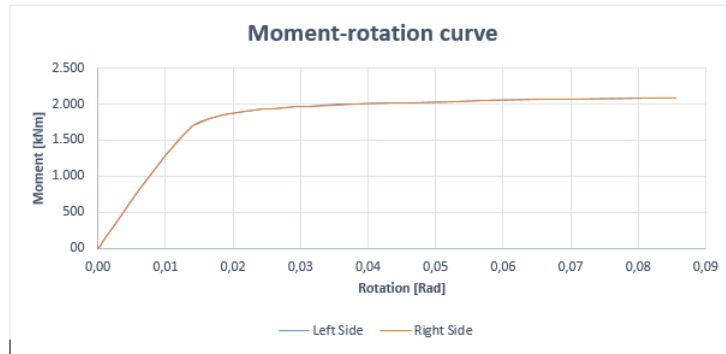


Figure 6.3: Comparison of Moment-Rotation curve of both sides of model (a)

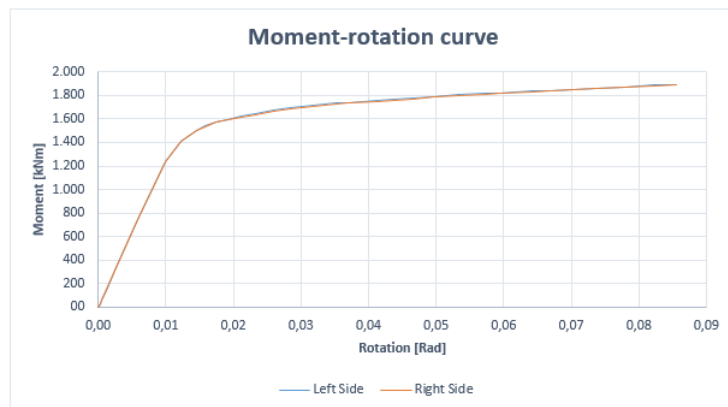


Figure 6.4: Comparison of Moment-Rotation curve of both sides of model (b)

This symmetry is present for every configurations tested in this paper.

6.2.1 Supplementary Web Plate Influence

For the 2 models (a) and (b), the only difference is in the presence of a second SWP of equal thickness in model (a). The shear area is thus increased for model (a). Model (a) is expected to have a higher plastic demand on the beam and a smaller plastic demand on the panel zone, while model (b) is expected to have a more balanced plastic demand between the beam and the panel zone.

The moment-rotation curves of the 2 models are shown hereafter ¹:

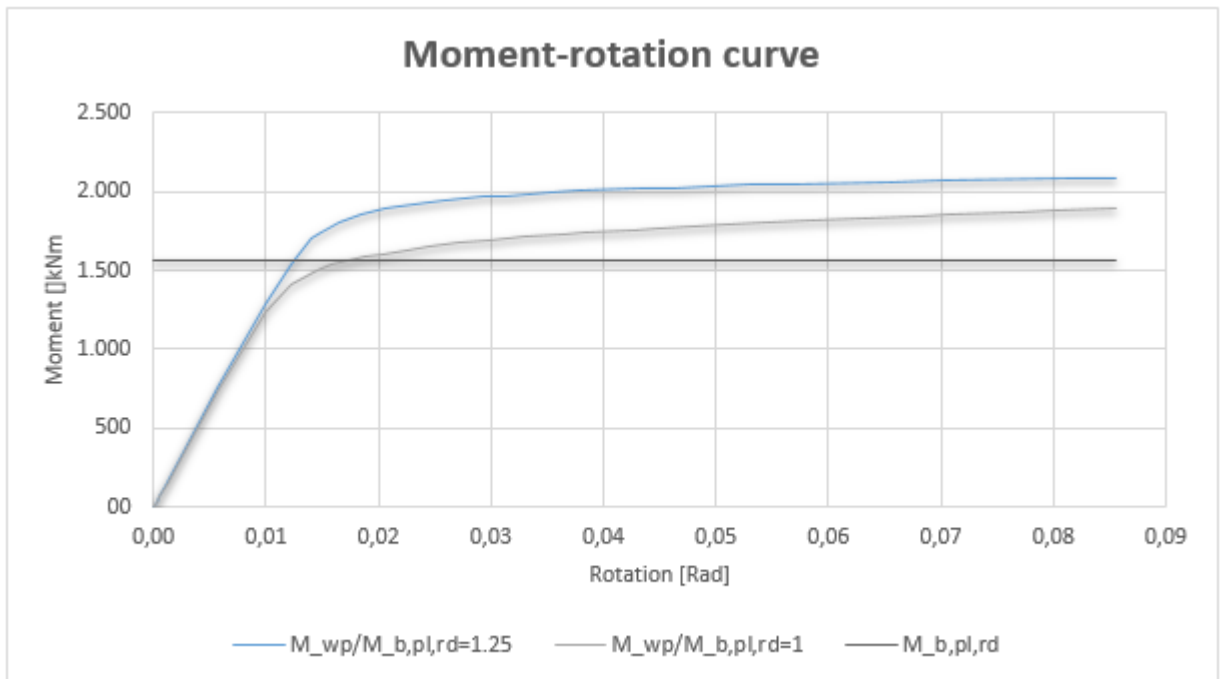


Figure 6.5: Influence of the supplementary web plate on the Moment-Rotation curve

¹The plastic moment resistance of the beam was calculated considering a material yield strength $f_y = 1.25 * 355 [MPa]$

We can make the following observation from these curves:

- The initial stiffness is not affected by the addition of SWP, i.e. the initial rigidity does not increase with the shear area. Which is in opposition with [11], where the augmentation of the shear area by the addition of SWP would increase the initial rigidity. However, this has to be taken carefully since we can only observe here that a second SWP of same thickness does not have an influence on the initial stiffness compared to the model with one SWP. It would be interesting to see the difference in initial stiffness with the same model without any SWP.
- We can see that for the model (a), the connection is still completely (or almost completely) in the elastic range when the value of the plastic moment resistance of the beam is attained. While for the model (b), the connection is already in the inelastic range at that level. Which as explained before would be beneficial in terms of energy dissipation. This is coherent with the design of these joints.
- We can see from the curves that the additional SWP only has an influence on the inelastic range. It increases the moment resistance of the connection. For a rotation of 0.03 Rad, the augmentation of the moment resistance due to the additional SWP is of 16 % (Model (a): $M_{j,Rd} = 1970kNm$, Model (b): $M_{j,Rd} = 1700kNm$). However, the presence of an additional SWP in the model (a) allowed for a bigger elastic range. This can be interesting when a strong panel design is desired (as in the Eurocode 8 for seismic actions).
- Although the joints were designed to be equal-strength, they seem to be full-strength when observing the curves. This potential overestimation of the connection moment resistance can be attributed, as explained in [12], to :
 - The residual stresses in the welds (not considered in the FE model)
 - The tolerances in the dimensions of the sections and the geometrical imperfections in the experimental results used to validate and calibrate the FE model.
 - The approximation used in incorporating the material stress-strain relationship into the FE model
 - Errors in determining the experimental initial rotational stiffness.
- We can see that for very large rotations of the joints, which will probably never be reached since rotations in seismic design are limited up to 6% – 7% at maximum, there seem to be a convergence of the 2 curves. It can be explained by the fact that for these very large deformations, the contribution of the deformation of the web panel on the total deformation of the connection is not as important and thus the benefit of the SWP decreases.

6.2.2 Continuity Plate Influence

As mentioned before, CP are used to prevent local flange and wand web overstress. They are expected to increase the stiffness of the compression and tension zone respectively of the column web panel.

They also increase the bending resistance of the column flange, they influence the T-Stab mechanism on the column side by changing the effective length. CP increase the tension resistance (tension zone) and the compression resistance (compression zone) of the column web panel.

According to the Eurocode, from Equation 4.29, it can be seen that if CP are used in both tension and compression zone of the CWP, the shear resistance of the CWP increases. This augmentation is calculated by considering the plastic contribution of the column flanges in the shear resistance of the CWP. Which, as pointed in [9], leads to an overestimation of the column web panel resistance because it does not consider the initial stress state in the column flanges before they are mobilized in the response and considering the full plastic capacity of the column flanges.

As explained earlier, for one same joint geometry, 4 different CP configurations were tested (No CP, and CP of thicknesses equal to 0.5 , 1 , 1.5 the thickness of the beam flange).

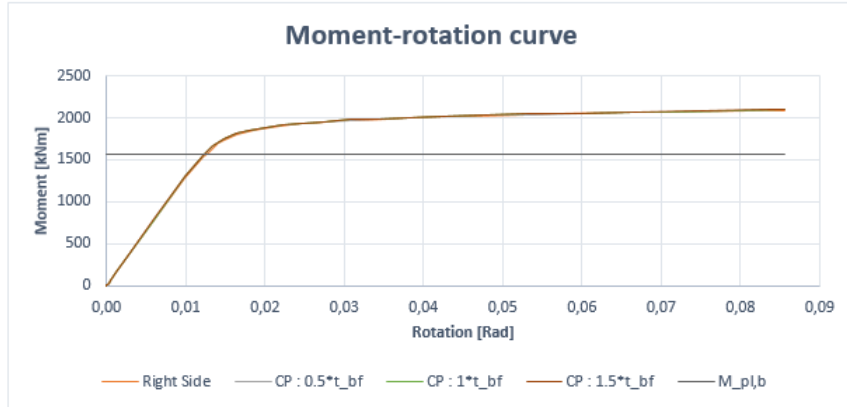


Figure 6.6: Comparison of Moment-Rotation curve for different CP thicknesses of model (b)

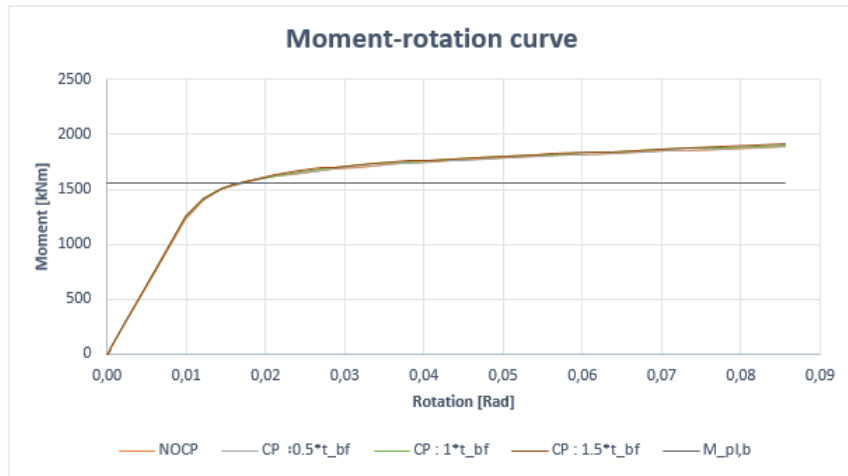


Figure 6.7: Comparison of Moment-Rotation curve for different CP thicknesses of model (b)

From these curves, we can observe that the continuity plates seem to not have any influence of the behavior of the connection. It could be due to the fact that CP increase the plastic rotation of the column web panel for very big plastic demand of the column web panel. These levels of plastic demand of the CWP have not been reached for these models. Thus, the CP do not show any significant contribution to the behavior of the joint.

6.3 Results and Comparison with the Component Method

Since the joint typologies that were tested in this study are not fully covered by the Eurocode, some adjustments have been made in order obtain the most accurate moment-rotation curve of the joint with the component method. This different approach is the one of the EQUALJOINT project. Although several differences exist, which will not be covered here (See EQUALJOINT project), one important difference is worth being noticed: unlike the limitation of the Eurocode to only consider the contribution of one SWP (even if 2 are present) to the shear area of the column web panel, the contribution of both SWP will be considered here.

A comparison with the American procedure would have been interesting too but these joints with 6 bolts on the compression side and 6 bolts on the tension side are not covered by the AISC.

Hereafter, on Figure 6.8, are represented the moment-rotation curves of the 3 different configurations of SWP for the Equal strength IPE600-HEB650 joint without any continuity plate ($M_{wp}/M_{pl,b,rd} = 0.75$; $M_{wp}/M_{pl,b,rd} = 1$; $M_{wp}/M_{pl,b,rd} = 1.25$):

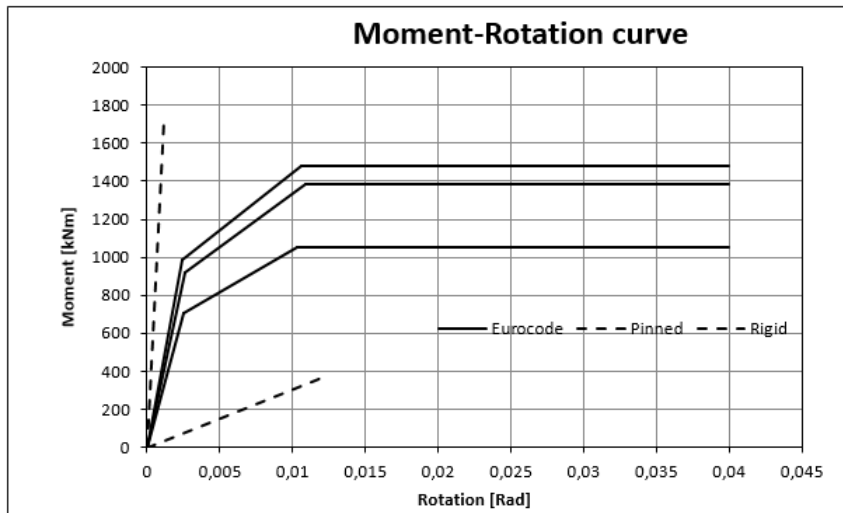


Figure 6.8: Moment Rotation curves obtained from component method

The following observations can be made from this graph:

- The joints are all semi-rigid, i.e. having their initial stiffness between the two limits from the Eurocode (Rigid and pinned).
- The initial stiffness of the joint increases with the shear area. Which is in agreement with [11], where the augmentation of the shear area by the addition of SWP would increase the initial rigidity. Compared to the joint without any supplementary web plate, the increase in initial stiffness with one SWP of 7 mm is of 24.7 % , and the increase with two SWP of 7 mm is of 46.4 %. While the increase in shear area, in comparison with the joint without SWP, is of 30.6 % for one SWP and of 61.2 % for two SWP. The initial stiffness increases almost proportionally with the shear area.
- The stiffness of the inelastic range (before attaining the moment resistance of the joint) is 24.7 % bigger with one SWP and 33.5 % bigger with two SWP. The contribution of the second SWP is then lower than the contribution of the first one.
- The moment resistance of the joint increases with the shear area. Again, comparing to the configuration without any SWP, the joint with one SWP

has an increase in the joint moment resistance of 31.2 %, while the joint with two SWP has an increase of 40.2 %.

The resistance has increased proportionally with the shear area for one SWP. However, the contribution of the second SWP is much smaller.

Obviously, a comparison of both methods with the real behavior of the joint obtained from experimental tests would be the best. But due to the lack of experimental tests, we now compare the results from the component method to the ones from the finite element analysis ². :

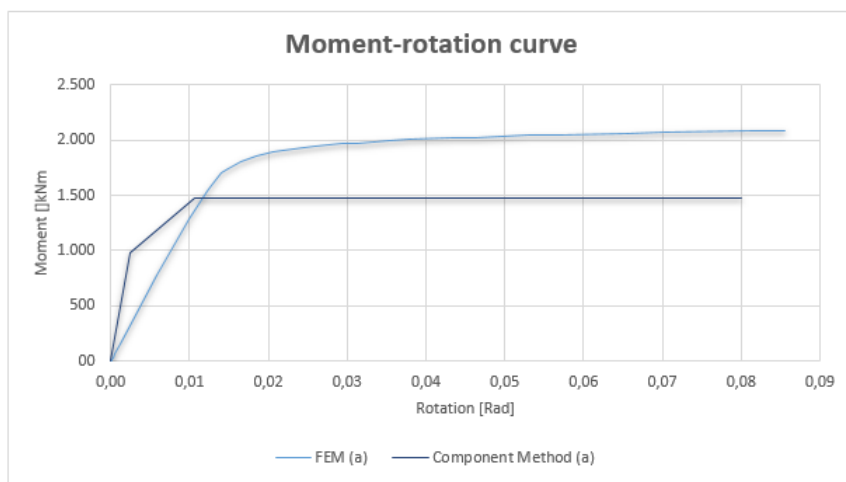


Figure 6.9: Comparison Component Method - FEA, model (a)

²The component method results were extended to a rotation of 0.08 Rad for comparison purpose only.

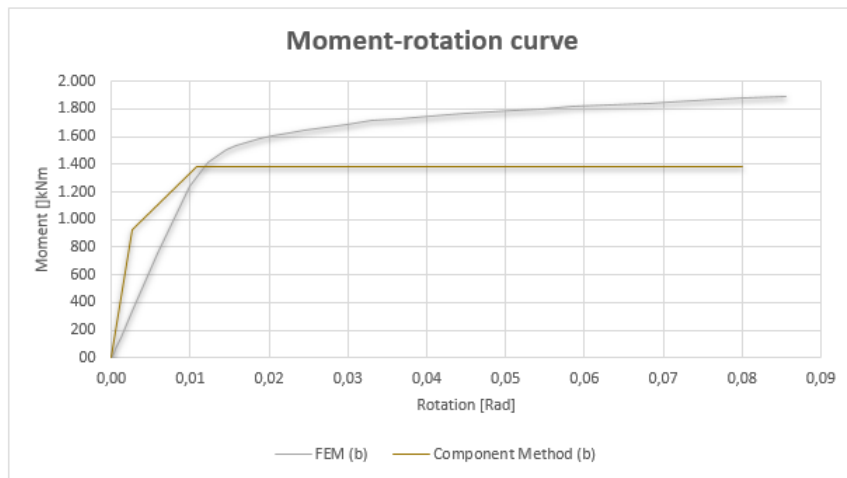


Figure 6.10: Comparison Component Method - FEA, model (b)

Some interesting observation can be made from these graphs:

- The component method used here give initial stiffness higher than the finite element analysis. They are 2.72 times higher for model (b) and 3.2 times higher for model (a).
- The joint moment resistance is higher in both FEA in comparison with the component method. The FE model (a) has a moment resistance 41% higher than the one obtained with the component method, while the FE model (b) has a moment resistance 37 % higher.
The differences in the increment of moment resistance for the 2 joints between the FE method and the component method are almost equal.
- The joint with 2 SWP, in comparison to the joint with one SWP, has an increase of the moment resistance of 6.8 % when evaluated with the component method, and of 10.1 % when evaluated with the FE method.
Here again, the two methods show some similarities.

Although there are some differences between the 2 methods in terms of initial stiffness and moment resistance, the 2 methods showed some agreements in the moment resistance differences between the 2 joint configurations. However they failed to do so in terms of initial stiffness, the FEM showing no differences in the initial stiffness.

The finite element method, as explained in [12] and already mentioned here before, will not be able to represent the exact real behavior of the joint due to :

- The residual stresses in the welds (not considered in the FE model)

- The tolerances in the dimensions of the sections and the geometrical imperfections in the experimental results used to validate and calibrate the FE model.
- The approximation used in incorporating the material stress-strain relationship into the FE model
- Errors in determining the experimental initial rotational stiffness.

All these reasons play a role in the difference between the 2 methods compared. However, the component method is also an inexact method, i.e. it does not represent the exact real behavior of the joint. Thus, as said before, further comparison of these results with experimental tests on the joints analyzed would be extremely interesting.

6.4 Cost Evaluation

Naturally, the reinforcement can enhance the connection stiffness and/or strength, but it comes at a cost. Indeed, when thinking of adding one or more stiffener to our connection, we have to evaluate if it is beneficial in a structural point of view, but also in an economical point of view.

From the analysis of the results previously made, it is obvious that adding CP is not advantageous. However, considering that if the panel zone was submitted to very large shear deformations, CP would have a beneficial effect on the behavior of the joint, it is still relevant to evaluate their price.

For the SWP, it could be very interesting to evaluate their cost because they can allow the panel zone to remain elastic (as desired in Eurocode 8). Therefore, no permanent deformation would be present after the seismic action. Which in a economical point of view could be beneficial since in case of retrofit of the structure, it would be harder and more expensive to renovate the column web panel, rather than to do the retrofit of the beam. We will now thus evaluate the cost of the different stiffeners added in our study (CP and SWP) :

In order to evaluate the price of such reinforcement, many different criteria have to be taken into account: the quantity of steel, its quality, the quantity of welding, the quality of welding, the place where the welding is realized,... However, it was possible to obtain an average price³, comprising all these parameters, of 6euros/kg of steel S355.

Knowing that the density of steel is 7850 [kg/m³], we can calculate the volume needed for our reinforcement and find the total mass needed, which will then give us the price for each reinforcement:

Table 6.9: Cost Evaluation

| Reinforcement | CP(9.5mm) | CP(19mm) | CP(28.5mm) | CP(9.5mm) | CP(19mm) | CP(28.5mm) | SWP(7mm) |
|--------------------------|----------------------|----------|------------|---------------|----------|------------|----------|
| | Welded on column web | | | Welded on SWP | | | |
| Volume [m ³] | 0.00078 | 0.00157 | 0.00235 | 0.00074 | 0.00149 | 0.00224 | 0.00411 |
| Masse [kg] | 6.17 | 12.34 | 18.51 | 5.87 | 11.75 | 17.63 | 32.27 |
| Price [euros/piece] | 38 | 75 | 112 | 36 | 71 | 106 | 194 |

It is quite clear that continuity plate are not advantageous in our case. However, further studies in order to evaluate their effect for joints submitted to large shear deformation would be needed.

For the supplementary web plate, since the Eurocode 8 requires no yielding of the panel zone, the addition of the second SWP is necessary, and the structural benefits outweigh the cost of such a reinforcement. But, if yielding of the panel zone is allowed (as allowed in the AISC), the gain in moment resistance is not as profitable

³This price is an average price that was given by the Belgian society Franki

since in both cases the moment resistance of the joint is larger than the flexural resistance of the adjacent beam. Again, further study in order to evaluate the gain obtained from the configuration without any SWP would be relevant. And additional study on the benefits of SWP on weaker panel zone (weaker column) would also be interesting.

Chapter 7

Conclusion

In this study, one bolted extended stiffened joint (IPE600-HEB650) has been tested numerically under monotonic loading. Different reinforcements have been added (Continuity plate and supplementary web plate) in order to investigate their influence on the column web panel zone.

Some conclusions could be made from the results:

- For the joint investigated, the CP did not have any significant influence. However, this is most probably due to the small shear deformation that the column web panel are submitted to (strong column having one or two SWP). Therefore, further studies on weaker column (other joint configurations) and on the same column without any SWP would be needed in order to evaluate the influence of the CP.
- The addition of the second SWP on the joint investigated increased the moment resistance of the joint, but did not have any influence on the initial stiffness. It allowed the increase of the elastic range of the joint, which can be interesting when the designer does not want the panel zone to yield (As desired in Eurocode 8 [3]).
However additional studies in order to compare the results obtained with the same joint without any SWP would be interesting. As well as other numerical analysis on other joint geometry.
- The finite element analysis showed an overestimation of the moment resistance obtained by the FEA and an underestimation of the initial stiffness, in comparison with the component method.
However, none of these methods describes exactly the real behavior of the joint.
Therefore, experimental tests on the joints analyzed would allow a better understanding of the limitations of the two methods used in this study.

List of Figures

| | | |
|------|---|----|
| 3.1 | Advantages and disadvantages of models to obtain the rotational joint behaviour.), ([13]) | 12 |
| 3.2 | Principal characteristics of current models to obtain the rotational behaviour of a joint.), ([13]) | 12 |
| 3.3 | Geometries of J1 and J3 series), ([10]) | 14 |
| 3.4 | Connections chosen for the EVD determination), ([10]) | 14 |
| 3.5 | Cyclic behavior and failure mode of cyclic specimens, 1), ([11]) . . | 15 |
| 3.6 | Cyclic behavior and failure mode of cyclic specimens, 2), ([11]) . . | 16 |
| 3.7 | Description of the CWP Tests), ([11]) | 16 |
| 3.8 | Different mathematical representations of the ($M_j - \Theta$) curve: (a) linear; (b) bi-linear; (c) multi-linear (tri-linear); (d) nonlinear.), ([13]) | 18 |
| 3.9 | Moment-Rotation Envelopes, ([14]) | 19 |
| 3.10 | Comparison between Experimental and Computed Curves, ([14]) | 19 |
| 3.11 | Joint Modeling Reflecting (a) Actual Behavior and (b) Simplified Modeling, ([14]) | 20 |
| 3.12 | Identification of dissipative components, ([19]) | 21 |
| 3.13 | EEP-CYC 01 Moment-Rotation curve, ([19]) | 22 |
| 3.14 | Energy dissipation of specimen EEP-CYC 01, ([19]) | 23 |
| 3.15 | Comparison between model and experimental dissipated energy, ([20]) | 24 |
| 3.16 | Hysteretic moment-rotation ($M - \Phi$) model of the extended end-plate connection, ([23]) | 25 |
| 3.17 | Joint rotation definition , ([23]) | 25 |
| 4.1 | Four-bolt stiffened configuration, (Chapter 6, [4]) | 27 |
| 4.2 | Four-bolt stiffened geometry, (Chapter 6, [4]) | 28 |
| 4.3 | Summary of Four-Bolt Extended Stiffened End-Plate Yield Line Mechanism Parameter, (Chapter 6, [4]) | 29 |
| 4.4 | Summary of Four-Bolt Extended Column Flange Yield Line Mechanism Parameter, (Chapter 6, [4]) | 31 |
| 4.5 | Classification of joints by stiffness, (Chapter 5, [2]) | 36 |
| 4.6 | Full Strength Joint, (Chapter 5, [2]) | 37 |
| 4.7 | Type of Joint Model, (Chapter 5, [2]) | 37 |

| | | |
|------|---|----|
| 4.8 | Joints components to be evaluated, (<i>Chapter 2, [30]</i>) | 38 |
| 4.9 | Connection Geometry, (<i>Chapter 2, [30]</i>) | 39 |
| 4.10 | T-Stub Failure Modes, (<i>[31]</i>) | 41 |
| 4.11 | Length of Equivalent T-stub of a Stiffened Column Flange in Bending, (<i>[31]</i>) | 41 |
| 4.12 | Transformation parameter β , (<i>Chapter 5, [2]</i>) | 43 |
| 4.13 | Effective Width β , (<i>[30]</i>) | 44 |
| 4.14 | Shear forces in Column Web Panel, (<i>[30]</i>) | 45 |
| 4.15 | Tension and compression resistances contributing to moment resistance, (<i>[30]</i>) | 46 |
| 4.16 | Tension and shear bolts, (<i>[30]</i>) | 47 |
| 4.17 | Spring model for multi bolt-rows end-plate joints, (<i>[31]</i>) | 48 |
| 4.18 | Principal stress distribution in the rib, (<i>[29]</i>) | 50 |
| 4.19 | Definition of rib cross section, (<i>[29]</i>) | 52 |
| 4.20 | Equivalent stress model, (<i>[29]</i>) | 52 |
| 4.21 | Supplementary web plate, (<i>Chapter 6, [2]</i>) | 54 |
| | | |
| 5.1 | Details of the setup), (<i>[25]</i>) | 56 |
| 5.2 | Section AA' of setup, (<i>[28]</i>) | 56 |
| 5.3 | Plastic stress - strain diagram for S355, (<i>[33]</i>) | 59 |
| 5.4 | Plastic stress - strain diagram for Bolts 10.9, (<i>[33]</i>) | 59 |
| 5.5 | Difference between nominal and net area of several bolt types, (<i>[33]</i>) | 60 |
| 5.6 | Meshed Bolt, (<i>[33]</i>) | 60 |
| 5.7 | ABAQUS Model (For the current project) | 61 |
| 5.8 | Bolt load definition and the effect of Clamping on the End Plate, [<i>33</i>] | 62 |
| 5.9 | Test Specimen and loading arrangement, [<i>25</i>] | 63 |
| 5.10 | Details of connection, [<i>25</i>] | 64 |
| 5.11 | Detailed dimensions of the connection, [<i>25</i>] | 64 |
| 5.12 | Material Properties, [<i>25</i>] | 64 |
| 5.13 | Failure mode comparison between experimental and FEA (Case 1), Experimental : [<i>25</i>] , FEA : [<i>33</i>] | 65 |
| 5.14 | Moment-rotation curve comparison (Case 1), [<i>25</i>] | 65 |
| 5.15 | Failure mode comparison between experimental and FEA (Case 2), Experimental : [<i>25</i>] , FEA : [<i>33</i>] | 66 |
| 5.16 | Moment-rotation curve comparison (Case 2), [<i>25</i>] | 66 |
| | | |
| 6.1 | Example of FE Model (IPE600-HEB650 with CP and SWP.), (<i>Abaqus</i>) 71 | |
| 6.2 | Meshing detail of a model (IPE600-HEB650 with CP and SWP.), (<i>Abaqus</i>) | 72 |
| 6.3 | Comparison of Moment-Rotation curve of both sides of model (a) . | 73 |
| 6.4 | Comparison of Moment-Rotation curve of both sides of model (b) . | 73 |
| 6.5 | Influence of the supplementary web plate on the Moment-Rotation curve | 74 |

| | | |
|------|---|----|
| 6.6 | Comparison of Moment-Rotation curve for different CP thicknesses of model (b) | 76 |
| 6.7 | Comparison of Moment-Rotation curve for different CP thicknesses of model (b) | 77 |
| 6.8 | Moment Rotation curves obtained from component method | 78 |
| 6.9 | Comparison Component Method - FEA, model (a) | 79 |
| 6.10 | Comparison Component Method - FEA, model (b) | 80 |

List of Tables

| | | |
|-----|------------------------------------|----|
| 5.1 | Units for ABAQUS | 57 |
| 6.1 | Equal Strength | 68 |
| 6.2 | Partial Strength | 68 |
| 6.3 | IPE 360 Equal Strength | 69 |
| 6.4 | IPE 360 Partial Strength | 70 |
| 6.5 | IPE 450 Equal Strength | 70 |
| 6.6 | IPE 450 Partial Strength | 70 |
| 6.7 | IPE 600 Equal Strength | 70 |
| 6.8 | IPE 600 Partial Strength | 71 |
| 6.9 | Cost Evaluation | 82 |

Bibliography

- [1] CEN EN 1993-1-1 *Eurocode 3: Design of steel structures: Part 1-1 General rules and rules for buildings*, (2005).
- [2] CEN EN 1993-1-8 *Eurocode 3: Design of steel structures: Part 1-8 Design of joints*, (2005).
- [3] CEN EN 1998-1-1 *Eurocode 8: Design of structures for earthquake resistance - Part 1: General rules, seismic actions and rules for buildings*, (2005).
- [4] ANSI/AISC 358-10 *Prequalified Connections for Special and Intermediate Steel Moment Frames for Seismic Applications*, (American Institute of Steel Construction, 2010).
- [5] ANSI/AISC 360-10 *Specification for Structural Steel Buildings*, (American Institute of Steel Construction, 2010).
- [6] AISC Steel Design Guide *Extended End-Plate Moment Connections Seismic and Wind Application*, (Second Edition 2004).
- [7] O.S.Bursi, J.P. Jaspart, *Calibration of a Finite Element Model for Isolated Bolted End-Plate Steel Connections*, (1997).
- [8] J.M. Castro, A.Y. Elghazouli, B.A. Izzuddin, *Modelling of the panel zone in steel and composite moment frames*, (Engineering Structures 27 (2005) 129 – 144).
- [9] J.M. Castro, F.J. Dávila-Arbona, A. Y. Elghazouli, *Seismic Design Approaches for Panel Zone in Steel Moment Frames*, (Journal of Earthquake Engineering, 2008).
- [10] J.M. Castro, H. Augusto, C. Rebelo, L. S. da Silva *Assessment of Key Parameters for Displacement-Based Seismic Design of Steel Moment Frames with Partial Strength Connections*.
- [11] A. L. Ciutina, D. Dubina, *Column Web Stiffening of Steel Beam-to-Column Joints Subjected to Seismic Actions*,.

- [12] C. Díaz, M. Victoria, P. Martí, O. M. Querin, *FE Model of Beam-to-Column extended End-Plate Joints*, (Journal of Constructional Steel Research, 2011).
- [13] C. Díaz, M. Victoria, P. Martí, O. M. Querin, *Review on the modelling of joint behaviour in steel frames*, (Journal of Constructional Steel Research, 2010).
- [14] D. Dubina, A. Ciutina, A. Stratan *Cyclic Tests of Double-Sided Beam-To-Column Joints*,.
- [15] C. Faella, V. Piluso, G. Rizzano, *A New Method to Design Extended End Plate Connections and Semirigid Braced Frames*, (J. Construct. Steel Res. Vol. 41, No. 1, pp. 61-91, 1997).
- [16] J.P. Jaspart, *General report: session on connections*, (Journal of Constructional Steel Research 55 (2000) 69 - 89).
- [17] Gun Jin Yun, Jamshid Ghaboussi, Amr S. Elnashai, *A new neural network-based model for hysteretic behavior of materials*, (INTERNATIONAL JOURNAL FOR NUMERICAL METHODS IN ENGINEERING , Int. J. Numer. Meth. Engng 2008; 73:447 - 469).
- [18] K. D. Kim, M. D. Engelhardt, *Monotonic and cyclic loading models for panel zones in steel moment frames*, (Journal of Constructional Steel Research 58 (2002) 605 - 635).
- [19] F. Iannone, M. Latour, V. Piluso, and G. Rizzano, *Experimental Analysis of Bolted Steel Beam-to-Column Connections: Component Identification*, (Journal of Earthquake Engineering, 15:214 - 244, 2011).
- [20] M. Latour, V. Piluso, and G. Rizzano, *Cyclic Modeling of Bolted Beam-to-Column Connections: Component Approach*, (Journal of Earthquake Engineering, 15:537 - 563, 2011).
- [21] M. Mofid, M.R.S. Mohammadi, S.L. McCabe, *Analytical Approach on End-plate Connection: Ultimate and Yielding Moment*,.
- [22] G. Rizzano, *Seismic Design of Steel Frames with Partial Strength Joints* , (Journal of Earthquake Engineering, 10:5, 725 - 747, 2008)
- [23] Gang Shi, Yongjiu Shi, Yuanqing Wang, *Behaviour of end-plate moment connections under earthquake loading*, (Engineering Structures 29, 703 - 716, 2007)
- [24] Emmett A. Sumner, Thomas M. Murray, *Behavior of Extended End-Plate Moment Connections Subject to Cyclic Loading*, (Journal of Constructional Steel, 2002)

- [25] Y. Shi, G. Shi, Y. Wang, *Experimental and theoretical analysis of the moment-rotation behaviour of stiffened extended end-plate connections*, (Journal of Constructional Steel Research 63, 1279 - 1293, 2007)
- [26] G. Terracciano, G. Della Corte, G. Di Lorenzo, R. Landolfo, *Simplified Methods of Analysis for End-Plate Beam-to-Column Joints*,
- [27] Meng Wang, Yongjiu Shi, Yuanqing Wang, Gang Shi, *Numerical study on seismic behaviors of steel frame end-plate connections*, (Journal of Constructional Steel Research 90 (2013) 140 - 152)
- [28] M. Zimbru, *Numerical Investigation of Seismic Behavior of Steel Stiffened Extended End Plate Connections* (2015).
- [29] Lee C-H, *Seismic design of rib-reinforced steel moment connections based on equivalent strut model*, (Journal of Structural Engineering, September 2002, 128 ; 1121 - 1129).
- [30] Steel Construction Institute, The British Constructional Steelwork Association Limited *Joints in Steel Construction : Moment-Resisting Joints to Eurocode 3*.
- [31] Adam, SKILLS - Steel construction industry lifelong learning support *Moment Connections - Part 1*.
- [32] SIMULIA *Abaqus-CAE User's Manual*.
- [33] R. Landolfo, M. D'Aniello, R. Tartaglia, S. Costanzo, G. Ambrosino, *Procedures and Assumptions and Definition of Numerical Quality Control Procedures*, (University of Naples Federico II, 2015).
- [34] G. Brandonisio, A. De Luca, E. Mele, *Shear strength of panel zone in beam-to-column connections*, (University of Naples Federico II, 2011).

Nomenclature

| | |
|-------------------|---|
| β | transformation parameter |
| η | equivalent strut area factor |
| γ_{M0} | the partial safety factor for resistance of cross-sections |
| γ_{M1} | partial safety factor for resistance of members |
| γ_{M2} | the partial safety factor for bolts |
| ω | reduction factor to allow for the interaction with shear in the column web panel (EN 1993-1-8 Table 6.3) |
| ρ | reduction factor for plate buckling (EN 1993-1-8 6.2.6.2(1)) |
| $\theta_{com,Ed}$ | the maximum coexisting longitudinal compression stress in the column web (due to axial force and bending moment). In most of the cases, the reduction factor is equal to 1. However, it can conservatively be taken as 0.7. |
| A_B | nominal cross sectional area of the selected bolt diameter |
| A_c | column cross-sectional area |
| A_s | tensile stress area of the bolt |
| A_{Be} | Effective area of the threads |
| $A_{effective}$ | area of the threaded region |
| A_{gross} | gross cross section of the shank |
| A_{vc} | shear area of the column (For rolled I and H sections) |
| b | Base |
| $b_{eff,c,wc}$ | effective width of the column web in compression |

| | |
|-----------------|--|
| $b_{eff,t,wb}$ | effective width of the beam web in tension; it is equal to the effective length of equivalent T-stub representing the end-plate in bending for an individual bolt-row or bolt-group |
| $b_{eff,t,wc}$ | effective width of the column web in tension (for a single bolt-row); It is taken as equal to the smallest of the effective lengths l_{eff} (individually or as a part of group of bolts) given in EN 1993-1-8 § 6.2.6.3 Table 6.5 |
| $b_{eff,t,wc}$ | effective width of the column web in tension; for bolted connection it is equal to the effective length of equivalent T-stub representing the column flange |
| d_0 | hole diameter for a bolt |
| d_B | nominal diameter of the bolt |
| d_b | beam depth |
| d_c | depth of the column |
| d_s | distance between the centerlines of the stiffeners |
| E | the Young's modulus |
| e_1 | end distance from the center of a bolt hole to the adjacent end of any part |
| f | stiffness correlation factor taken as 0.55 |
| F_i | specified LFRD bolt tensile strength |
| F_u | specified minimum tensile strength of end-plate of column flange material |
| f_u | ultimate tensile strength of the material of either: the end-plate or the column flange |
| F_v | nominal shear strength of bolts Table J3.2 of the AISC LRFD Specification (AISC, 1999) |
| f_{actual} | actual stress |
| F_c | column flange material yield strength |
| $f_{effective}$ | effective stress |
| $F_{t,ep,Rd}$ | End-plate in bending resistance |
| $F_{t,fc,Rd}$ | Column flange in bending resistance |
| $F_{t,Rd}$ | design tension resistance of bolt |

| | |
|---------------|---|
| $F_{t,wb,Rd}$ | Beam web in tension resistance |
| $F_{t,wc,Rd}$ | Column web in transverse tension resistance |
| f_{ub} | ultimate tensile strength for the bolt |
| F_{yb} | specified minimum yield stress of beam material |
| F_{yp} | end-plate material yield strength |
| F_{yr} | yield strength of the rib |
| F_{ys} | specified minimum yield stress of stiffener material |
| h | depth of the section; for haunched beam, it is the depth of the fabricated section |
| h_i | distance from the centerline of the beam compression flange to the centerline of the i^{th} tension bolt row |
| h_r | distance between bolt-row r and the center of compression |
| h_{st} | stiffener height |
| I_b | moment of inertia of the beam about the strong axis |
| k_b | Elastic stiffens of the bolt |
| k_c | distance from outer face of the column flange to web toe of fillet |
| $k_{eff,r}$ | effective stiffness coefficient for bolt-row r taking into account the stiffness k_i for the basic components |
| k_{eq} | equivalent stiffness coefficient |
| k_{wc} | reduction factor (EN 1993-1-8 6.2.6.2(2)) |
| L_b | bolt elongation length, taken as equal to the grip length (total thickness of material and washers), plus half the sum of the height of the bolt head and the height of the nut |
| L_c | clear distance, in the direction of the force, between the edge of the hole and the edge of the adjacent hole or edge of the material |
| L_s | Length of the bolt shank |
| l_{eff}' | smallest of the effective lengths l'_{eff} (individually or as a part of group of bolts) given for this bolt-row given in EN 1993-1-8 §6.2.6.5 Table 6.6 |

| | |
|----------------|--|
| l_{eff} | smallest of the effective lengths l_{eff} (individually or as a part of group of bolts) given for this bolt-row given in EN 1993-1-8 § 6.2.6.3 Table 6.5 |
| L_{tg} | Length of the threaded portion |
| $M_{c,Rd}$ | design moment resistance of beam cross-section, reduced if necessary to allow for shear (EN 1993-1-1 6.2.5) |
| $M_{j,Rd}$ | Design plastic moment resistance of the joint |
| $M_{pl,b,Rd}$ | design plastic moment resistance of Beam |
| $M_{pl,fc,Rd}$ | design plastic moment resistance of a column flange |
| $M_{pl,st,Rd}$ | design plastic moment resistance of a stiffener |
| M_{uc} | moment at the face of the column |
| M_{wp} | Moment resistance of Column Web Panel (Shear resistance times lever arm) |
| N | thickness of beam flange plus 2 times the groove weld reinforcement leg size |
| N' | normal interaction force |
| n_b | number of bolts at the compression flange |
| n_i | number of inner bolts |
| n_o | number of outer bolts |
| p_1 | spacing between centers of bolts in a line |
| P_r | Required strength |
| P_y | axial yield strength of the column |
| Q | tangential interaction force |
| s_f | leg length of the fillet weld between the compression flange and the end plate |
| t_f | thickness of an equivalent T-stub flange ($t_f = t_{fc}$ or $t_f = t_p$) |
| t_p | end-plate thickness |
| t_{fb} | beam flange thickness |
| t_{fc} | column flange thickness |
| t_{wb} | beam web thickness |

| | |
|-------------|---|
| t_{wc} | column web thickness |
| V_u | shear at the plastic hinge |
| $V_{bw,Rd}$ | the shear buckling resistance of the web |
| Y_p | end-plate yield line mechanism parameter obtained from Figure 4.3 |
| Y'_p | column flange yield line mechanism parameter obtained from Figure 4.4 |
| z | lever arm |
| z_{eq} | equivalent lever arm |